

The Bacterial Cytoskeleton Modulates Motility, Type 3 Secretion, and Colonization in *Salmonella*

David M. Bulmer¹, Lubna Kharraz¹, Andrew J. Grant², Paul Dean¹, Fiona J. E. Morgan², Michail H. Karavolos¹, Anne C. Doble¹, Emma J. McGhie³, Vassilis Koronakis³, Richard A. Daniel¹, Pietro Mastroeni², C. M. Anjam Khan^{1*}

1 Centre for Bacterial Cell Biology, Institute for Cell and Molecular Biosciences, The Medical School, University of Newcastle, Newcastle, United Kingdom, **2** Department of Veterinary Medicine, University of Cambridge, Cambridge, United Kingdom, **3** Department of Pathology, University of Cambridge, Cambridge, United Kingdom

Abstract

Although there have been great advances in our understanding of the bacterial cytoskeleton, major gaps remain in our knowledge of its importance to virulence. In this study we have explored the contribution of the bacterial cytoskeleton to the ability of *Salmonella* to express and assemble virulence factors and cause disease. The bacterial actin-like protein MreB polymerises into helical filaments and interacts with other cytoskeletal elements including MreC to control cell-shape. As *mreB* appears to be an essential gene, we have constructed a viable $\Delta mreC$ depletion mutant in *Salmonella*. Using a broad range of independent biochemical, fluorescence and phenotypic screens we provide evidence that the *Salmonella* pathogenicity island-1 type three secretion system (SPI-1-T3SS) and flagella systems are down-regulated in the absence of MreC. In contrast the SPI-2 T3SS appears to remain functional. The phenotypes have been further validated using a chemical genetic approach to disrupt the functionality of MreB. Although the fitness of $\Delta mreC$ is reduced *in vivo*, we observed that this defect does not completely abrogate the ability of *Salmonella* to cause disease systemically. By forcing on expression of flagella and SPI-1 T3SS *in trans* with the master regulators FlhDC and HilA, it is clear that the cytoskeleton is dispensable for the assembly of these structures but essential for their expression. As two-component systems are involved in sensing and adapting to environmental and cell surface signals, we have constructed and screened a panel of such mutants and identified the sensor kinase RcsC as a key phenotypic regulator in $\Delta mreC$. Further genetic analysis revealed the importance of the Rcs two-component system in modulating the expression of these virulence factors. Collectively, these results suggest that expression of virulence genes might be directly coordinated with cytoskeletal integrity, and this regulation is mediated by the two-component system sensor kinase RcsC.

Citation: Bulmer DM, Kharraz L, Grant AJ, Dean P, Morgan FJE, et al. (2012) The Bacterial Cytoskeleton Modulates Motility, Type 3 Secretion, and Colonization in *Salmonella*. PLoS Pathog 8(1): e1002500. doi:10.1371/journal.ppat.1002500

Editor: Mark Stevens, Roslin Institute, United Kingdom

Received: May 24, 2011; **Accepted:** December 7, 2011; **Published:** January 26, 2012

Copyright: © 2012 Bulmer et al. This is an open-access article distributed under the terms of the Creative Commons Attribution License, which permits unrestricted use, distribution, and reproduction in any medium, provided the original author and source are credited.

Funding: This work was supported by Medical Research Council UK (www.mrc.ac.uk) grant (G0801212) to CMAK. LK was supported by a Ford Foundation of America (www.fordfoundation.org) PhD studentship with CMAK. ACD is supported by a Medical Research Council (UK)(www.mrc.ac.uk) PhD studentship to CMAK and RAD. AJG is supported by a Medical Research Council (UK) (www.mrc.ac.uk) grant (G0801161). The funders had no role in study design, data collection and analysis, decision to publish, or preparation of the manuscript.

Competing Interests: The authors have declared that no competing interests exist.

* E-mail: anjam.khan@ncl.ac.uk

Introduction

Salmonellae remain major global pathogens causing a broad spectrum of disease ranging from gastroenteritis to typhoid fever [1,2]. The emergence of multidrug resistant salmonellae is complicating the management of disease [3,4]. Hence, there is an urgent need to identify novel bacterial targets for the development of new antimicrobial agents or vaccines to combat infection.

The view that bacteria do not possess a cytoskeleton has radically changed in recent years with the discovery of intracellular filamentous protein assemblies with cell-shape defining function [5]. Although there is little primary sequence identity between eukaryotic cytoskeletal proteins and those in prokaryotes, proteins with actin- and tubulin-like structural motifs have been identified in bacteria. Bacterial cytokinesis is dependent on FtsZ which contains a structural fold mirroring tubulin. FtsZ displays similar dynamic properties to tubulin and is able to polymerise unidirectionally in a GTP-dependent manner to produce poly-

meric filaments [6,7]. Polymers of FtsZ are able to assemble into a transient helical structure and subsequently form a ring-like structure around the circumference of the mid-cell [8]. This Z-ring is required for recruiting proteins for the assembly of the cell division complex [8]. The intermediate filament-like protein crescentin determines the vibroid shape of *Caulobacter crescentus* cells [9].

The bacterial proteins MreB, Mbl, and ParM display the structural and dynamic properties of eukaryotic actin [10]. Amongst these proteins, MreB is the most homologous to actin in terms of primary sequence, structure, and size [11,12]. The most conserved region of this actin-superfamily is the ATPase domain. MreB can polymerise into helical filamentous structures important for cell morphology. Live cell microscopy in *Bacillus subtilis* revealed that MreB forms large cables which follow a helical path close to the cytoplasmic membrane [5]. An equivalent MreB protein has been found in *Escherichia coli*. When MreB is depleted, rod-shaped *B. subtilis* and *E. coli* cells become spherical [5,13–15]. In *C. crescentus* MreB has been implicated to play a role in the

Author Summary

Salmonella are major global pathogens responsible for causing food-borne disease. In recent years the existence of a cytoskeleton in prokaryotes has received much attention. In this study the *Salmonella* cytoskeleton has been genetically disrupted, causing changes in morphology, motility and expression of key virulence factors. We provide evidence that the sensory protein RcsC detects changes at the cell surface caused by the disintegration of the bacterial cytoskeleton and modulates expression of key virulence factors. This study provides insights into the importance of the integrity of the bacterial cytoskeleton in the ability of *Salmonella* to cause disease, and thus may provide a novel target for antimicrobial drugs or vaccines.

control of cell polarity [16]. In rod-shaped bacteria the MreB polymeric structures control the localisation of cell wall growth by providing a scaffold for enzymes involved in cell wall assembly [17].

The MreB operon in *E. coli* and *B. subtilis* encodes for a number of additional genes, which do not possess any similarity to actin [18]. These include the cellular membrane proteins MreC and MreD, which also have a helical disposition. MreC forms a dimer and interestingly in *C. crescentus* MreC is localised in spirals in the periplasm [19]. Recent studies by Rothfield and colleagues provide convincing evidence to suggest that in *E. coli* MreB, MreC and MreD form helical structures independently of each other [20]. Using affinity purification and bacterial two hybrid assays, MreC and MreD appear to interact together [13]. In *E. coli* there is evidence to suggest that MreB interacts with MreC, but this may not be the case in *Rhodobacter sphaeroides* or *C. crescentus* [21]. As well as playing a key role in cell morphogenesis, MreB also has a pivotal function in chromosome segregation [22–24]. Adding the MreB inhibitor A22 [*S*-(3,4-Dichlorobenzyl) isothiourea] to synchronised cultures of *C. crescentus* inhibited segregation of GFP-tagged chromosomal origins [22]. However MreB may not function in chromosome segregation in *Bacillus* [15]. Recently another helically distributed cytoplasmic membrane protein which interacts with MreB named RodZ has been identified [25–27]. Cellular components including the RNA degradosome and lipopolysaccharide have also been identified to be localised in helical structures within the cell [28,29].

In spite of these major advances in our understanding of the structure and organization of the bacterial cytoskeleton, there are major gaps in our knowledge of its role in bacterial pathogenicity. In this study we wished to gain insights into understanding the function of the bacterial cytoskeleton in the pathogenicity of *Salmonella*.

Materials and Methods

Ethics Statement

The *in vivo* experiments were covered by a Project License granted by the Home Office under the Animal (Scientific Procedures) Act 1986. This license was approved locally by the University of Cambridge Ethical Review Committee.

Culture Conditions

S. Typhimurium SL1344 and mutant derivatives used in this study are described in Table 1. Strains were routinely grown in Luria-Bertani (LB) broth with appropriate antibiotics at the following concentrations: (kanamycin 50 $\mu\text{g ml}^{-1}$), ampicillin (100 $\mu\text{g ml}^{-1}$ or 30 $\mu\text{g ml}^{-1}$ for pNDM220). A22 (Calbiochem)

was added at 10 $\mu\text{g ml}^{-1}$. Bacteria were grown overnight in 5 ml LB, before 25 μl of culture was used to inoculate 25 ml of fresh LB in a 250 ml flask and grown at 37°C shaking (200 rpm) unless otherwise stated. ΔmreC was maintained in media containing 100 μM IPTG, however for phenotypic testing this was removed unless otherwise mentioned.

For the SPI-1 T3S studies cells were grown overnight in LB before subculturing 1/100 into 25 ml fresh LB and growing at 37°C for approximately 5 hrs with good aeration until $\text{OD}_{600\text{nm}} \sim 1.2$ in 250 ml flasks [30]. For the SPI-2 T3S studies cells were grown in SPI-2 induction media (100 mM Tris-base, 0.1% w/v casamino acids, 0.1% w/v glycerol, 10 μM MgSO_4 , 40 $\mu\text{g ml}^{-1}$ histidine, pH 5.8). Cells were grown overnight in LB before subculturing 1/100 in 25 ml SPI-2 inducing media before growing for 16 h at 37°C in 250 ml flasks before sampling.

Motility Assays

Cells were inoculated from a fresh LB plate onto the semi-solid motility agar (10 g l^{-1} Bacto-tryptone, 5 g l^{-1} NaCl, 3 g l^{-1} agar) and incubated upright for a minimum of 5 h. Distinct zones of cell motility were measured and compared to WT SL1344 and non-motile SL1344 strains.

Chromosomal Gene Disruptions and Deletion Mutants

Chromosomal gene deletions were constructed using the lambda Red method as described previously [31], before transducing the mutation into a genetically clean parent strain using bacteriophage P22*int*. In the case of ΔmreC and ΔmreD the mutations were transduced into a parent strain containing pTK521 (*lac-mreBCD E. coli*) to complement the mutation in the presence of 100 μM isopropyl beta-D-1-thiogalactopyranoside (IPTG). Gene deletion primers typically encompassed the first and final 20 bases of the coding sequence of the respective gene were synthesised. However, as the *mreC* and *mreD* gene coding sequences overlap by a single base, to ensure only a single coding sequence was disrupted the respective *mreC* 3' primer and *mreD* 5' primer were moved internally into their coding sequence such as to produce no overlapping mutations. Gene deletions for the two-component systems (ΔqseF , ΔphoBR , ΔyjiGH , ΔbaeSR , ΔbasSR , ΔhydH , ΔqseBC , ΔtciDE , ΔcpxAR , ΔrcaA , ΔrcsB , ΔrcsC , ΔrcsD , ΔrcsDB , and ΔrcsCBD), were constructed in SL1344 WT using classical lambda Red methods before transducing into the ΔmreC strain using bacteriophage P22*int*. Primers are listed in Table 2.

Construction of the MreB-GFP Fusion Vector

GFP was amplified from pZEP08 and cloned along with a new multiple cloning site into the *EcoRI* and *HindIII* sites of pBR322 to create pBR322GFP. *mreB* along with its natural promoter was amplified from genomic DNA and cloned into the *EcoRI* and *XbaI* sites of pBR322GFP, before the *mreB-gfp* fusion was subcloned from the pBR322*mreB-gfp* into pNDM220 using the *EcoRI* and *BamHI* sites.

Transcriptional Reporter Fusions

Flagella and SPI1 transcriptional reporter plasmids were transformed into SL1344 and ΔmreC mutant cells. Expression from the *lux* transcriptional reporters was measured during the growth cycle of 10^{-3} diluted overnight cultures cells grown in microtitre plates (200 μl total volume) for a minimum of 15 h at 37°C with periodic shaking. Optical density (600_{nm}) and relative luminescence was measured at 15 minute intervals using a Tecan Infinity200 luminometer. Samples were tested in triplicate, and repeated at least 3 times.

Table 1. Strains and plasmids.

Strain	Genotype	Reference
SL1344	Parent Strain	[69]
$\Delta mreC1$	SL1344 <i>mreC::kan</i>	This work
$\Delta mreD1$	SL1344 <i>mreD::kan</i>	This work
$\Delta mreC$	SL1344 <i>mreC::kan pTK521</i>	This work
$\Delta mreD$	SL1344 <i>mreD::kan pTK521</i>	This work
$\Delta SPI-1$	RM69 <i>SPI-1::kan</i>	[70]
$\Delta SPI-2$	12023 <i>ssaV::kan</i>	[71]
$\Delta flhDC$	LT2 <i>flhDC::kan</i>	[72]
$\Delta rcsA$	SL1344 <i>rcsA::kan</i>	This work
$\Delta rcsB$	SL1344 <i>rcsB::kan</i>	This work
$\Delta rcsC$	SL1344 <i>rcsC::cat</i>	This work
$\Delta rcsD$	SL1344 <i>rcsD::kan</i>	This work
$\Delta rcsF$	SL1344 <i>rcsF::kan</i>	This work
$\Delta rcsDB$	SL1344 <i>rcsDB::kan</i>	This work
$\Delta rcsCBD$	SL1344 <i>rcsCBD::kan</i>	This work
$\Delta mreC \Delta rcsA$	SL1344 <i>mreC::cat rcsA::kan</i>	This work
$\Delta mreC \Delta rcsB$	SL1344 <i>mreC::cat rcsB::kan</i>	This work
$\Delta mreC \Delta rcsC$	SL1344 <i>mreC::kan rcsC::cat</i>	This work
$\Delta mreC \Delta rcsD$	SL1344 <i>mreC::cat rcsD::kan</i>	This work
$\Delta mreC \Delta rcsDB$	SL1344 <i>mreC::kan rcsDB::cat</i>	This work
$\Delta mreC \Delta rcsCBD$	SL1344 <i>mreC::cat rcsCBD::kan</i>	This work
$\Delta mreC \Delta rcsF$	SL1344 <i>mreC::cat rcsF::kan</i>	This work
$\Delta mreC \Delta qseF$	SL1344 <i>mreC::kan qseF::cat</i>	This work
$\Delta mreC \Delta phoBR$	SL1344 <i>mreC::kan phoBR::cat</i>	This work
$\Delta mreC \Delta yjiGH$	SL1344 <i>mreC::kan yjiGH::cat</i>	This work
$\Delta mreC \Delta baeSR$	SL1344 <i>mreC::kan baeSR::cat</i>	This work
$\Delta mreC \Delta basSR$	SL1344 <i>mreC::kan basSR::cat</i>	This work
$\Delta mreC \Delta hydH$	SL1344 <i>mreC::kan hydH::cat</i>	This work
$\Delta mreC \Delta qseBC$	SL1344 <i>mreC::kan qseBC::cat</i>	This work
$\Delta mreC \Delta tctDE$	SL1344 <i>mreC::kan tctDE::cat</i>	This work
$\Delta mreC \Delta cpxAR$	SL1344 <i>mreC::kan cpxAR::cat</i>	This work
YVM004	SJW1103 <i>gfp-flhG</i>	[32]
YVM004 <i>mreC</i>	SJW1103 <i>gfp-flhG mreC::kan</i>	[32]
TH3724	<i>PflhDC::T-POP (DEL-25) flhC5213::MudJ</i>	[33]
Plasmid	Description	Reference
pBR322	Cloning vector	[73,74]
pBAD24	Cloning vector	[75]
pZEP08	GFP+ transcriptional fusion vector	[76]
pBR322- <i>gfp</i>	pBR322 with <i>gfp</i>	This work
pBR322- <i>mreBgfp</i>	pBR322 <i>gfp</i> with <i>mreB</i>	This work
pNDM220	Low copy cloning vector	[77]
pNDM220- <i>mreBgfp</i>	<i>mreBgfp</i> subcloned from pBR322- <i>mreBgfp</i>	This work
pKD13	Lambda Red template	[31]
pKD46	Lambda Red recombinase	[31]
pLE7	<i>gfpmreB</i>	[36]
pTK521	pNDM220 pA1/O4/O3:: <i>mreBCD</i>	[14]
pCS26	<i>luxCDABE</i> promoter reporter vector	[49]
pCS26- <i>hilA</i>	<i>hilA</i>	[49]
pCS26- <i>hilC</i>	<i>hilC</i>	[49]
pCS26- <i>hilD</i>	<i>hilD</i>	[49]

Table 1. Cont.

Plasmid	Description	Reference
pSB401	<i>luxCDABE</i> promoter reporter vector	[41]
pBA409	<i>sopB</i> promoter reporter	[41]
pRG34	pSB401- <i>fliA</i>	[41]
pRG38	pSB401- <i>flhD</i>	[41]
pRG46	pSB401- <i>fliC</i>	[41]
pRG51	pSB401- <i>flgA</i>	[41]
pMK1- <i>lux</i>	<i>luxCDABE</i> promoter reporter vector	[52]
pMK1- <i>lux-ssaG</i>	pMK1- <i>lux-ssaG</i>	This work
pBAD24- <i>hilA</i>	<i>hilA</i> inducible expression plasmid	This work
pBAD24- <i>rcsC</i>	<i>rcsC</i> complementation plasmid	This work

doi:10.1371/journal.ppat.1002500.t001

Construction of Complementation Plasmids

The *hilA* and *rcsC* open reading frames were amplified from SL1344 genomic DNA and cloned into the *EcoRI* and *XbaI* or the *EcoRI* and *HindIII* sites of pBAD24 to create pBAD*hilA* and pBAD*rcsC* respectively.

Protein Manipulation

Whole cell total protein samples were obtained by pelleting an appropriate volume of bacterial culture, followed by resuspension in SDS-loading buffer and boiling for 10 mins. Culture supernatants were filter sterilized (0.22 μm) and proteins were ammonium sulphate precipitated (4 g 10 ml⁻¹ supernatant) overnight at 4°C. Precipitated secreted proteins were resuspended in H₂O and then combined with an equal volume of sample buffer (Biorad). Whole cell and culture supernatant samples were run on 12% SDS/PAGE and transferred on Protran nitrocellulose transfer membranes (Schleicher & Schuell) using a wet transfer apparatus (Biorad). Western blot analysis was performed using polyclonal SipA, SipB, SipC or PrgH for testing SPI-1 T3S functionality, coupled with a goat anti-mouse horseradish peroxidase-labelled secondary antibody (Dako Cytomation). Detection was carried out using 4-chloro-1-naphthol (Sigma) according to the manufacturer's instructions.

In vivo Inoculation and Growth Curves

Female C57BL/6 mice were purchased from Harlan Olac Ltd., (Blackthorn, Bicester, UK). Mice were used when over eight weeks of age. Bacterial suspensions for injection were grown for 16 h as a stationary culture at 37°C in LB broth. Bacteria were diluted in PBS prior to injection into a lateral tail vein. Mice were killed by cervical dislocation and the livers and spleens aseptically removed. Each organ was homogenised (separately) in a Seward Stomacher 80 Biomaster (Seward) in 10 ml of distilled water and viable bacterial counts in the homogenate were assayed on pour plates of LB agar. Representative bacterial colonies were kept and re-tested for phenotypic changes.

Construction of Flagella Live Cell Imaging Strains

Wild type *Salmonella* SJW1103 cells with chromosomal N-terminal GFP fusion to *fliG* (YVM004) [32] were P22 transduced with the *mreC::kan* mutation to create YVM004 Δ *mreC*. This strain, along with the WT control, was subsequently transduced with a chromosomally-based inducible *flhDC* locus derived from TH2919 [33].

Visualisation of Type 3 Secretion Systems and Flagella

Cells were grown to the appropriate growth phase (mid-log for SPI-1 and flagella, or stationary phase for SPI-2) in relevant media (LB or SPI-2 inducing media). Flagella visualisation strains (*fliG-gfp*), were mounted on 1% agarose beds for imaging. Samples for visualising the type 3 secretion apparatus were fixed in 4% paraformaldehyde diluted in PBS for 1 h before washing for 15 minutes in three changes of PBS. Samples were incubated with either α SipA, α SipB, α SipC, α SipD (SPI-1) or α SseB (SPI-2) antibodies diluted 1:1000 in PBS for 3 h with gentle agitation. Samples were subsequently washed in PBS before incubating in 1:1000 Alexa Fluor 488 conjugated goat anti-rabbit antibody (Invitrogen-Molecular Probes, Paisley, U.K.), washed for 30 mins in fresh PBS before mounting onto agarose beds.

Tissue Immunostaining for Fluorescence Microscopy

Half of each organ was fixed overnight in 4% paraformaldehyde diluted in PBS, washed for 90 min in three changes of PBS and then immersed in 20% sucrose (in PBS) for 16 h at 4°C before being embedded in Optimal Cutting Temperature (OCT) (Raymond A Lamb Ltd, Eastbourne, U.K.) in cryomoulds (Park Scientific, Northampton, U.K.). Samples were frozen and stored at -80°C. 30 μm sections were cut, blocked and permeabilised for 10 min in a permeabilising solution containing 10% normal goat serum and 0.02% Saponin in PBS (Sigma, Poole, UK). Sections were stained with 1:1000 dilution of rat anti-mouse CD18⁺ monoclonal antibody (clone M18/2, BD Pharmingen), together with a 1:500 dilution of rabbit anti-LPS O4 agglutinating serum (Remel Europe Ltd), for 16 h at 4°C. Subsequently, sections were washed in PBS then incubated with 1:200 Alexa Fluor 568-conjugated goat anti-rat antibody (Invitrogen-Molecular Probes, Paisley, U.K.) and a 1:1000 dilution of Alexa Fluor 488-conjugated goat anti-rabbit antibody (Invitrogen-Molecular Probes, Paisley, U.K.). All sections were mounted onto Vecta-bond-treated glass slides (Vector Laboratories Ltd.) using Vecta-shield containing DAPI (Vector Laboratories Ltd.).

Microscopy

All phase contrast and fluorescence images were captured using an Andor iXon^{EM+} 885 EMCCD camera coupled to a Nikon Ti-E microscope using a 100x/NA 1.4 oil immersion objective. Images were acquired with NIS-ELEMENTS software (Nikon) and processed using ImageJ. Fluorescence images were decon-

Table 2. PCR primers.

Primer	Sequence (5'-3')
<i>mreC</i> -P1	GGATTGCTCCTCTCCGACGCGAGAATACGCATAGCCTGTGTAGGCTGGAGCTGCTTC
<i>mreC</i> -P4	CATCAGGCGCTCATTGGCGACGCGGTGAACCTCTCCGGATTCCGGGGATCCGTCGACC
<i>mreC</i> 5	ATACGGCAGGATTATCCCT
<i>mreC</i> 3	GCGCAATAAGAAACGAGAGC
<i>mreD</i> -P1	GGCGCGACCACGCCCTGCGCGTGCGCCGGGAGGGTAGTGTAGGCTGGAGCTGCTTC
<i>mreD</i> -P4	GGGGAACCGAAGCAAGATACAGAGTTGCATATCGACCTATTCCGGGGATCCGTCGACC
<i>mreD</i> 5	ATCAACGCAACCATCGCCTT
<i>mreD</i> 3	TCAATAATTCCTGGCGACGC
<i>qseBC</i> P1	GTTAACTGACGGCAACGCGAGTTACCGCAAGGAAGAAGAGGTGTAGGCTGGAGCTGCTTC
<i>qseBC</i> P4	AAATGTGCAAAAGTCTTTTGCCTTTTGGCAAAGTCTCTGATTCCGGGGATCCGTCGACC
<i>qseBC</i> 5'	ACATCGCCTGCGGCGACAAG
<i>qseBC</i> 3'	GCGGTGCGGTGAAATTAGCA
<i>rcsA</i> P1	GTAAGGGGAATTATCGTTACGCATTGAGTGAGGGTATGCCGTGTAGGCTGGAGCTGCTTC
<i>rcsA</i> P4	AATTGAGCCGACTGGAGGTACATTGCCAGTCCGGATGTCATTCCGGGGATCCGTCGACC
<i>rcsA</i> 5'	GATTATGGTGAGTTATTAG
<i>rcsA</i> 3'	CGAGAAGGCGGAGCAGGACT
<i>rcsB</i> P1	GCCTACGTCAAAGCTTGCTGTAGCAAGGTAGCCAATACGTGTAGGCTGGAGCTGCTTC
<i>rcsB</i> P4	ATAAGCGTAGCGCCATCAGGCTGGGTAACATAAAAGCGATATTCCGGGGATCCGTCGACC
<i>rcsB</i> 5'	CGTGAGAAAGATGCTCCAGG
<i>rcsB</i> 3'	TGAGTCGACTGGTAGGCTG
<i>rcsC</i> P1	GTCACACTCTATTTACATCCTGAGGCGGAGCTTCGCCCTGTGTAGGCTGGAGCTGCTTC
<i>rcsC</i> P4	TTTTACAGGCCGGACAGGCGACGCCCATCCGGCATTATTTCCGGGGATCCGTCGACC
<i>rcsC</i> 5'	CGTCATTTACCGCTACCTTA
<i>rcsC</i> 3'	GGCCTACCAGTCGACTCATC
<i>rcsD</i> P1	CCTTCACCTTCAGCGTTGCTTTTACAGGTCGTAACATAAAGTGTAGGCTGGAGCTGCTTC
<i>rcsD</i> P4	ACCTTGCTACAGCAAGCTTTTACAGTAGGCGTCAATGTCGATTCCGGGGATCCGTCGACC
<i>rcsD</i> 5'	TTCATTACCCTTTATACTGC
<i>rcsD</i> 3'	CATATTGTTTCATGTATTGGG
<i>rcsF</i> P1	TTCAATATCTGGCAATTAGAACATTCATTGAGGAAATATTGTGTAGGCTGGAGCTGCTTC
<i>rcsF</i> P4	GGGGAGCGAATAACGCCGATTTGATCAAACGAAAGCTGCATTCCGGGGATCCGTCGACC
<i>rcsF</i> 5'	TCATTTATGCAAGCTCCTGA
<i>rcsF</i> 3'	CGGCGAATTTTCTTTATAG
<i>rcsCBD</i> P1	GTCACACTCTATTTACATCCTGAGGCGGAGCTTCGCCCTGTGTAGGCTGGAGCTGCTTC
<i>rcsCBD</i> P4	CCTTCACCTTCAGCGTTGCTTTACAGGTCGTAACATAAATCCGGGGATCCGTCGACC
<i>rcsCBD</i> 5'	CGTCATTTACCGCTACCTTA
<i>rcsCBD</i> 3'	TTCAATTACCCTTTATACTGA
<i>rcsDB</i> P1	CCTTCACCTTCAGCGTTGCTTTTACAGGTCGTAACATAAAGTGTAGGCTGGAGCTGCTTC
<i>rcsDB</i> P4	ATAAGCGTAGCGCCATCAGGCTGGGTAACATAAAAGCGATATTCCGGGGATCCGTCGACC
<i>rcsDB</i> 5'	TTCATTACCCTTTATACTGC
<i>rcsDB</i> 3'	TGAGTCGACTGGTAGGCTG
<i>phoBR</i> P1	ATGGCGCGCATTGATAACTAACGACTAACAGGGCAAATTTGTGTAGGCTGGAGCTGCTTC
<i>phoBR</i> P4	CATCCGCTGGCTTATGGAAAGTTATACTTACGAAAGGCAAATTCGGGGATCCGTCGACC
<i>phoBR</i> 5'	TGTCATAAATCTGACGCATA
<i>phoBR</i> 3'	CTGCAAAGAAAATAAGCCAG
<i>qseF</i> P1	GGGCGCCGTCGCCGTCACAAGATGAGGTAACGCCATGATAAGTGTAGGCTGGAGCTGCTTC
<i>qseF</i> P4	TTAAACGTAACATATTTTCGCGCTACTTTACGGCATGAAAAATTCGGGGATCCGTCGACC
<i>qseF</i> 5'	CAAACCCGCGACGTCTGAAG
<i>qseF</i> 3'	GTCGCTGTGTTTGTATCGG
<i>cpxAR</i> P1	CGCCTGATGACGTAATTTCTGCTCGGAGGTACGTAAACAGTGTAGGCTGGAGCTGCTTC
<i>cpxAR</i> P4	CGAGATAAAAATCGGCTGCATTTCGAGGCCGATGGTTTATTCCGGGGATCCGTCGACC

Table 2. Cont.

Primer	Sequence (5'-3')
<i>cpxAR</i> 5'	GTAAGTCATGGATTAGCGA
<i>cpxAR</i> 3'	CTCCCGTAAATCTCGACGG
<i>tctDE</i> P1	AATTCCTTTCAATGCGGCAGAACTTTACAGGATGTGATGTGTAGGCTGGAGCTGCTTC
<i>tctDE</i> P4	TTTTGTAAACGTGCTTTACCGCTGACACATTTGCCGCAATTCGGGGATCCGTCGACC
<i>tctDE</i> 5'	TGTTAAACAATAACCTTTC
<i>tctDE</i> 3'	GTCACACCTCAAGATGCGAC
<i>yjiGH</i> P1	TTCTGCTCCCAGCTCCGGCCTGCGTCAACACCTGTTTCTGTGTAGGCTGGAGCTGCTTC
<i>yjiGH</i> P4	TAAACTCCGCGGGGATAAATCAGGCATGATAACTCCTTAATTCCGGGGATCCGTCGACC
<i>yjiGH</i> 5'	TCAAATTTATTTCTCTTTT
<i>yjiGH</i> 3'	GTGCGCACCTGTAATAAGG
<i>HydH</i> P1	TCTGTTGCCAGTGATAGCGAGACAACAGGATTAACAAGGGTGTAGGCTGGAGCTGCTTC
<i>HydH</i> P4	GTAACGACATTGGCTGGCGGCCATTGAGCGTGAGCAAAAATCCGGGGATCCGTCGACC
<i>HydH</i> 5'	TAAAGCGCGGTCTTTACTA
<i>HydH</i> 3'	CTGGGACGGCAGTTCAGCC
<i>BasS</i> P1	CTACATGCTGGTTGCCACTGAGGAAAGCTAAGTGAGCCTGGTGTAGGCTGGAGCTGCTTC
<i>BasS</i> P4	AGTTTTATCTATGTGTGGGTCACGACGTATTAACGCCTGATTCCGGGGATCCGTCGACC
<i>BasS</i> 5'	CGCACGGTTCGCGGGTTTGG
<i>BasS</i> 3'	GTAGTGTGCTGATTGTCAGC
<i>BaeSR</i> P1	TGGTCATTTACGCGGCTAAAAGGAGCCTGTAATGAAAGTCGTGTAGGCTGGAGCTGCTTC
<i>BaeSR</i> P4	ATATCGTCTTACGACCTTGTATTGTATGCCAATAATCAATTCGGGGATCCGTCGACC
<i>BaeSR</i> 5'	CCGCGTGCCGAACGATACAC
<i>BaeSR</i> 3'	CAGAATAGCGTTGGCGGAAA
pEGFP5	GCG GAATTC AGGTACCCCGGGCCATGGTCTAGAATGGTGAGCAAGGGCGAGG
pEGFP3	GCG AAGCTT TTACTTGTACAGCTCGTCC
<i>mreB5</i> Eco	GCG GAATTC GCAGATGTTGTCAACACATC
<i>mreB3</i> Xba	GCG TCTAGACT CTTCGCTGAACAGGTCGCC
<i>ssaG5</i> Eco	GCG GAATTC CGACAGTATAGGCAATGCCG
<i>ssaG3</i> Bam	GCG GGATCCC CACTAATTGTGCAATATCC
BAD <i>hilA5</i>	GCG GAATTC CATGCCACATTTAATC
BAD <i>hilA3</i>	GCG TCTAGATT ACCGTAATTTAATC
BAD <i>rcsC5</i>	GCG GAATTC TTGAAATACCTTGCTTC
BAD <i>rcsC3</i>	GCG AAGCTT TTATGCCCGCTTTTACGTACCC

Bold indicates restriction enzyme recognition sites.

doi:10.1371/journal.ppat.1002500.t002

involved using Huygens Deconvolution software (Scientific Volume Imaging). Cell measurements were taken on a Nikon Ti-E microscope with NIS-ELEMENTS software. Immunofluorescence images from tissue sections were analysed multi-colour fluorescence microscopy (MCFM) using a Leica DM6000B Fluorescence microscope running FW4000 acquisition software.

Transepithelial Resistance and Bacterial Effector Translocation Assays

The effect of *Salmonella* infection on transepithelial resistance (TER) was determined for differentiated Caco-2 cells as previously described [34]. Briefly, the Caco-2 cells were grown on transwell inserts (Corning, UK) until differentiated (12–14 days), before the transepithelial resistance was measured for each well. *Salmonella* strains were then added to the cells at a multiplicity of infection (MOI) of 20, and the cells incubated for 4 h. TER measurements were taken every hour and the results given as a ratio of TER (t/

(t⁰) to show the percentage change in TER over the course of the experiment. Data were collated and analysed for statistical differences (Student's t-test) in Minitab.

Samples for the assay of translocated effector proteins were isolated from differentiated Caco-2 cells grown in 6 well plates after infection with an MOI of 20 for 4 h. Excess bacteria were washed off before the cells were solubilised in 0.01% Triton X-100 and centrifuged to remove bacteria and host cell membranes. The host cell cytoplasmic fractions were analysed by western blotting with α SipB antibody.

Results

In silico Identification of the *Salmonella* Actin Homologue *mreB*

We wished to identify and characterise putative *Salmonella* cytoskeletal gene homologues. A BLAST search of the *S.*

Typhimurium genome sequence database (www.ncbi.nlm.nih.gov) [35] for the known *E. coli* actin-homologue MreB identified a putative *mre* operon of high sequence identity. Comparison of the *Salmonella* genes to those of *E. coli* showed 100% (*mreB*), 88% (*mreC*) and 94% (*mreD*) homology at amino acid level, comparisons of these same genes to those in *B. subtilis* revealed sequence homologies of 57%, 24% and 27% respectively.

MreB Proteins Are Helically Localised

In order to determine the localisation of MreB in *Salmonella*, vectors expressing N and C terminal fusions of MreB to GFP were used. The N-terminal fusion plasmid has already been described [36], and we constructed a C-terminal fusion vector. Both constructs revealed a helical distribution of MreB along the long axis of the cell. The helices were discerned by assembling a series of z-stack images taken in successive planes by using Metamorph imaging and Huygens deconvolution software (Figure 1A).

Construction of *mre* Mutants

The *mreB* gene appears to be essential in bacteria including *Salmonella* (data not shown), and $\Delta mreB$ viable cells often contain compensatory mutations [37]. Each of the components of the cytoskeletal complex, for example MreB, MreC, or MreD, are essential for its function. As an alternative strategy to study the function of the cytoskeleton we therefore generated a *mreC* depletion strain under conditions designed to minimise selective pressures for undefined secondary compensatory mutations [37]. Using the lambda Red one-step gene disruption method, we successfully constructed a *mreC::kan* mutant in the *S. Typhimurium* wild-type strain SL1344 [31]. This mutation leaves intact the first gene in the operon *mreB*. Using bacteriophage P22_{int} the *mreC::kan* mutation was then transduced into a genetically “clean” SL1344 strain harbouring *plac-mre* operon (pTK521) [14] and the resulting strain designated $\Delta mreC$. The *plac-mre* operon is a low copy number plasmid expressing the *mre* operon from the IPTG-inducible *lac* promoter. The identity of the mutation was confirmed by PCR and DNA sequencing. Expression of MreC was assessed by western blotting in the mutant strains, revealing no detectable levels MreC unless complementation was induced (Figure S1). In addition to the $\Delta mreC$ mutant, the lambda Red method was used to generate $\Delta mreD$.

Morphology and Growth Rates

When the morphology of the $\Delta mreC$ mutant was examined microscopically, the cells were no longer rod-shaped but spherical (Figure 1B). Upon the addition of IPTG the morphology of the $\Delta mreC$ strain was restored to the wild-type rod shape. Under microscopic examination the $\Delta mreD$ mutant displays a similar morphological phenotype to the $\Delta mreC$. WT cells were measured to be on $1.61(\pm 0.49)$ μm in length and $0.75(\pm 0.17)$ μm in width, whereas the $\Delta mreC$ cells were $2.03(\pm 0.60)$ μm in length and $1.21(\pm 0.41)$ μm in width. Complementation of the $\Delta mreC$ mutant with 100 μM IPTG resulted in wild type shaped cells $1.82(\pm 0.44)$ μm in length and $0.78(\pm 0.24)$ μm in width. Measurements were taken from a minimum of 350 cells per strain. Growth rates of the strains were determined in LB media at 37°C revealing a ~50% increase in the lag phase of the $\Delta mreC$ mutants (Figure S2), which subsequently grow at a comparable rate to that of the wild type or complemented mutant strains during log phase.

Motility and Expression of Flagellin Subunits

The motility phenotype of $\Delta mreC$ was examined on semi-solid agar plates. In contrast to the isogenic parent, the $\Delta mreC$ cells were

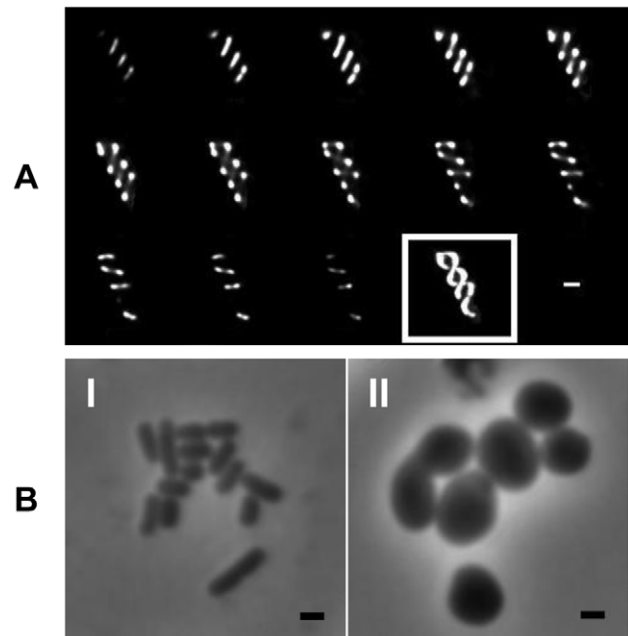


Figure 1. Localization and morphological role of the *S. Typhimurium* Mre proteins. (A) Fluorescence microscopy montage showing z-sections of MreB-GFP fusions in WT SL1344 revealing a helical distribution. Slices taken at 0.1 μm intervals on live cells in mid log phase going from left to right followed by maximum intensity projection (boxed). (B) Morphology of WT *S. Typhimurium* (I) and $\Delta mreC$ (II) reveal the mutant has changed from rod to round-shaped, with some heterogeneity in size noted. In all images the bar represents 1 μm .

doi:10.1371/journal.ppat.1002500.g001

no longer motile. Surprisingly, this motility defect has not been reported in either *E. coli* or *B. subtilis*. Cellular and secreted proteins of the parent SL1344 and $\Delta mreC$ were examined by SDS-PAGE and western blotting using antibodies directed against the phase-1 and phase-2 flagellin subunits FljC and FljB. Neither of these subunits were present in either the secreted or cellular proteins, explaining the inability of the cells to swim (data not shown). The non-motile phenotype was fully complementable *in trans* upon the addition of IPTG to the mutant strain harbouring pTK521 (Figure S3).

Expression of Flagella Genes

We observed that the *Salmonella* $\Delta mreC$ depletion strain was non-motile and failed to express flagella subunits FljC or FljB. The regulation and assembly of flagella in *Salmonella* is complex. Flagella genes are arranged into 14 operons and their transcription is organised into a regulatory hierarchy of early (class I), middle (class II), and late genes (class III) [38]. The class I *flhDC* operon is the master regulator, with FlhD and FlhC forming a heterotetramer that is required for transcriptional activation of the class II genes, which encode the hook-basal body complexes and the alternative sigma factor FliA (sigma₂₈). FliA alone or with FlhDC, activates expression of the class III operon genes, which encode the filament protein, hook-associated proteins, motor proteins, and chemotaxis proteins [39,40]. The class III genes are further subdivided into *fliA*-independent expression class IIIa or class IIIb [41]. In order to systematically investigate the mechanistic basis for the $\Delta mreC$ motility phenotype we have taken selected class I, II, and III regulated flagella gene promoter fusions to a luciferase reporter gene, and monitored their expression by luminescence in

wild type and $\Delta mreC$ strains. Constructs with *flhD* (class I), *fliA*, *flgA*, (class II), and *fliC* (class III) promoters fused to the luciferase reporter gene were used. The reporter plasmid pSB401 has a promoterless *luxCDABE* operon and was used as a control.

The class I *flhD* promoter displayed a reduction in the level of expression in $\Delta mreC$ compared to the wild-type strain suggesting the class I promoter has reduced activity. Notably greater changes in the expression profiles occur in other class II and class III genes. The class II promoters for the operons encoding the transcriptional regulators *fliAZ* and *flgAM* display significant reductions in expression levels in $\Delta mreC$ (Figure 2). As predicted from the western blotting data expression of the *fliC* class III promoter was significantly reduced. Collectively, the promoter-reporter activity data can account for the motility defect.

Expression of SPI-1 and SPI-2 Type 3 Secretion System Proteins

Type 3 secretion systems are essential for the virulence of a range of pathogens including *Salmonella* [42,43]. The secretion apparatus assembles into a supramolecular needle-complex. Secreted effector proteins in the bacterial cytoplasm traverse through the needle-complex and the bacterial multi-membrane envelope, directly into host cells [44–46]. The apparatus anchors to the cell envelope via a multi-ring base. *Salmonella* possess two T3SS's encoded by pathogenicity islands (SPI's). The SPI-1 T3SS is important for invasion of intestinal epithelial cells and the SPI-2 T3SS plays a central role in survival within the hostile environment of a macrophage. The SPI-1 T3SS system translocates virulence effector proteins into the cytosol of epithelial cells resulting in rearrangements of the actin cytoskeleton which enable *Salmonella* to invade [47]. To investigate whether the *mreC* mutation has an impact on SPI-1 T3SS, we used western blotting

to determine the presence and functionality of the system using antibodies to an apparatus protein PrgH as well as the effector proteins SipA and SipC, in both SL1344 and $\Delta mreC$. In contrast to the wild-type SL1344, the T3S structural and effector proteins were not expressed in the cellular or secreted fractions from the $\Delta mreC$ depletion mutant (Figure 3A). This suggests that SPI-1 T3SS in the $\Delta mreC$ mutant is not fully functional. The expression and secretion phenotypes were fully complementable *in trans* upon the addition of IPTG (data not shown).

The functional assembly of SPI-1 T3SS was also confirmed using transepithelial resistance (TER) assays in differentiated Caco-2 cells, showing a reduced ability to disrupt epithelial tight junctions in the $\Delta mreC$ mutant compared to the wild type strain (Figure 4).

To further assess the disruption of the functionality of the SPI-1 T3SS, a translocation assay was performed in Caco-2 cells infected with the strains. Host cell cytoplasmic proteins were probed for the bacterial effector protein SipB using western blotting (Figure S4). This revealed the inability of the $\Delta mreC$ mutants to infect host epithelia and disrupt their tight junctions. In addition, $\Delta mreC$ was fully complementable in this assay following IPTG induction.

The SPI-2 T3SS is pivotal for the establishment of the *Salmonella* containing vacuole (SCV) inside macrophages and subsequent survival [43]. We next investigated the effect of the $\Delta mreC$ mutation on the functionality of the SPI-2 T3SS. The strains were grown under SPI-2 inducing conditions and the T3S of the translocon protein SseB monitored. SseB together with SseC and SseD function as a translocon for other effector proteins and SseB is normally found associated with the outer surface of *Salmonella*. Thus membrane fractions were purified to monitor expression and T3S by western blotting. This revealed that in contrast to the SPI-2 negative control (*ssaV*), SseB was secreted and associated with the

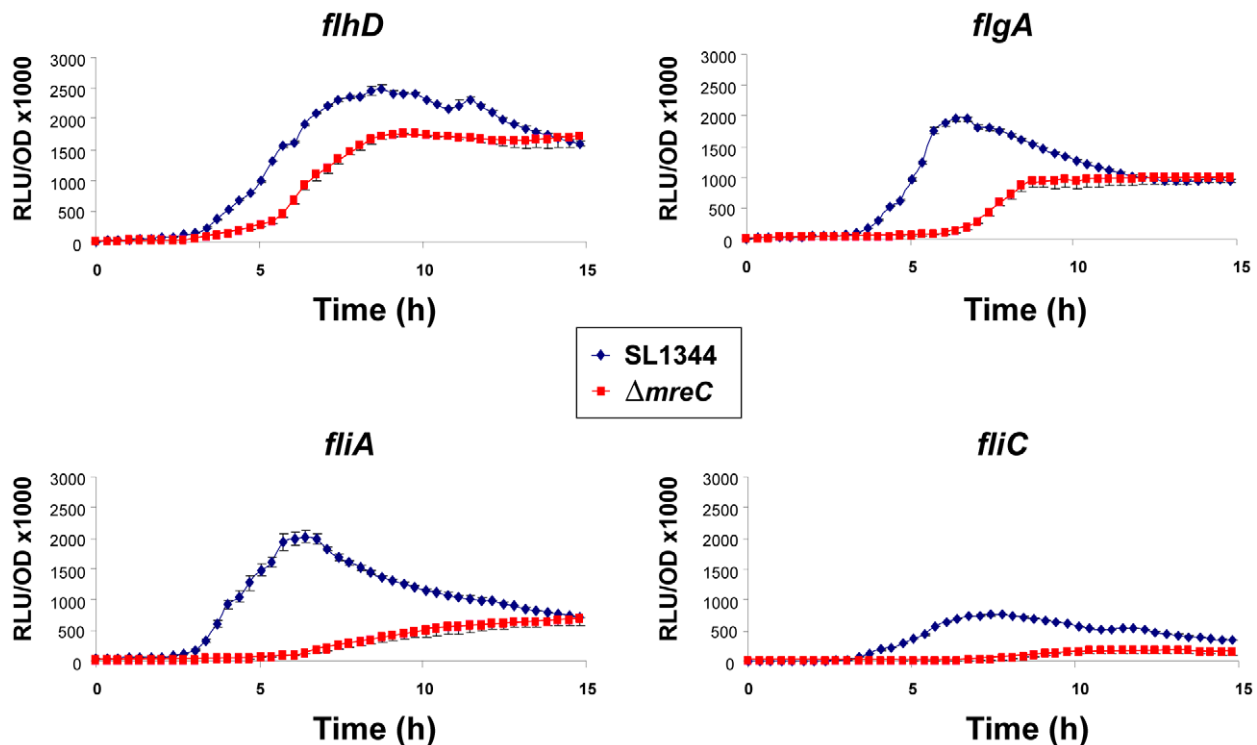


Figure 2. Impact of $\Delta mreC$ on the transcription of flagellar genes. Transcriptional expression profiles of *flhD*, *flgA*, *fliA* and *fliC* promoter reporters in WT SL1344 (blue diamonds) and $\Delta mreC$ (red squares) expressing the *Photobacterium luminescens* LuxCDABE luciferase. Experiments were repeated at least three times and error bars indicate standard deviation. doi:10.1371/journal.ppat.1002500.g002

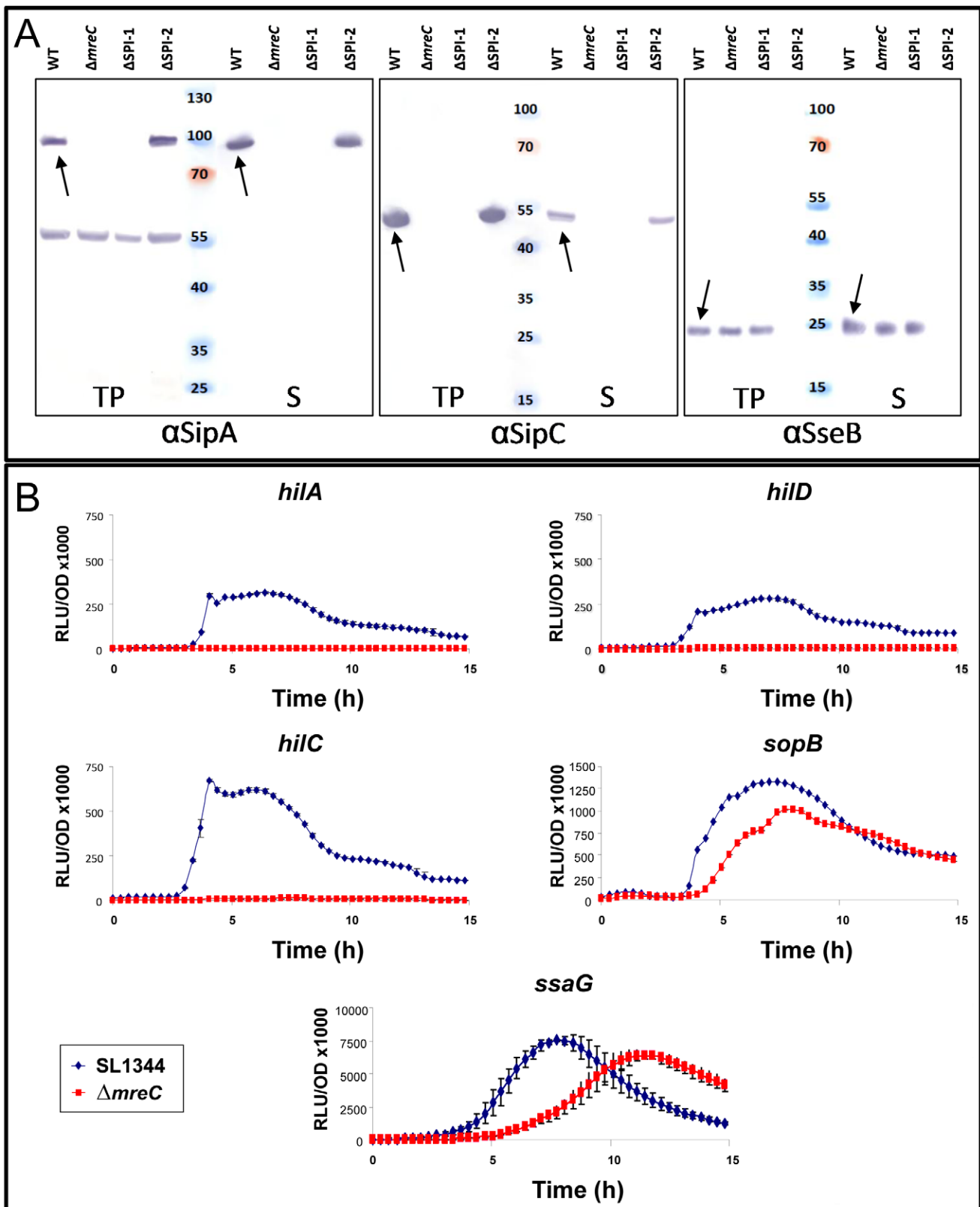


Figure 3. Expression of *Salmonella* SPI-1 and SPI-2 effector proteins in $\Delta mreC$. (A) Expression of SPI-1 proteins in WT SL1344, $\Delta mreC$, $\Delta SPI-1$, and $\Delta SPI-2$ mutants during SPI-1 inducing conditions as revealed by western blotting with polyclonal $\alpha SipA$ and $\alpha SipC$ antibodies. Expression of SPI-2 in WT SL1344, $\Delta mreC$, $\Delta SPI-1$, and $\Delta SPI-2$ mutants during SPI-2 inducing conditions as revealed by western blotting of membrane fraction samples with polyclonal $\alpha SseB$ antibody. Samples representing total proteins and secreted proteins are shown. Arrows indicate the respective protein bands. (B) Transcriptional expression profiles of *hilA*, *hilC*, *hilD*, *sopB* (SPI-1) and *ssaG* (SPI-2) promoter reporters in WT SL1344 (blue diamonds) and $\Delta mreC$ (red squares). Experiments were repeated at least three times and error bars indicate standard deviation. doi:10.1371/journal.ppat.1002500.g003

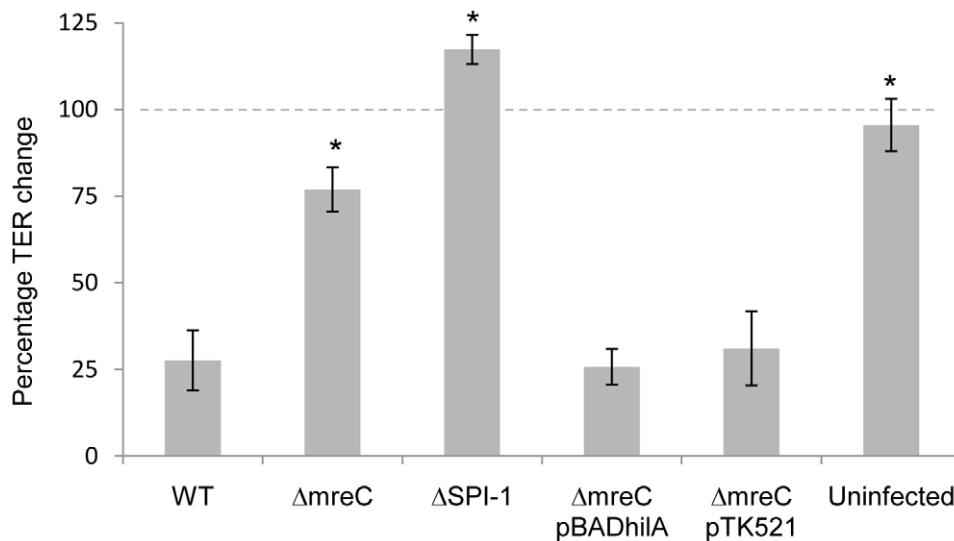


Figure 4. Percentage change in transepithelial resistance of differentiated Caco-2 cells after 4hr infection. TER of polarised Caco-2 monolayers exposed to *Salmonella* strains at an MOI of 20. TER change is expressed as a percentage alteration at 4hr compared to the initial value at time zero. Error bars indicate the standard deviations derived from at least three independent experiments. * Indicates statistical difference from WT ($p < 0.05$).

doi:10.1371/journal.ppat.1002500.g004

bacterial membrane surface in both the wild-type and $\Delta mreC$ strains (Figure 3A). This provides qualitative evidence to suggest that in contrast to the SPI-1 T3SS, the SPI-2 T3SS appears to remain functional.

Expression of SPI-1 and SPI-2 Type 3 Secretion System Regulatory Genes

Several environmental signals and transcriptional factors modulate expression of the SPI-1 T3SS. We wished to understand the mechanistic basis by which expression of the SPI1-T3SS is down-regulated. Within SPI-1 there are key transcriptional activators which regulate expression of SPI-1 genes: HilC, HilD, HilA, and InvF. Both HilC and HilD activate expression of SPI-1 genes by binding upstream of the master regulatory gene *hilA* to induce its expression [48]. HilA binds and activates promoters of SPI-1 operon genes encoding the type 3 secretory apparatus, several secreted effectors, and the transcriptional regulator InvF. InvF activates expression of effector genes inside SPI1 and also effector genes outside SPI-1 such as *sopB* and *sopE* [47].

Expression of selected SPI-1 T3SS genes was monitored using transcriptional promoter reporters in $\Delta mreC$, using constructs harbouring the *hilA*, *hilC*, *hilD*, *invF* and *sopB* promoters fused to the promoterless *luxCDABE* operon that produces light in response to gene expression [49–51]. Each construct was introduced into both wild-type SL1344 and $\Delta mreC$ depletion mutant, and the level of expression of the promoters in these strains monitored by luminescence assays. WT SL1344 and $\Delta mreC$ cells harbouring pCS26 or pSB401 vectors alone were used as controls, and did not produce any luminescence as expected. The reporter assays revealed that the SPI-1 transcription factor gene promoters for *hilA*, *hilC*, *hilD*, and *invF* were completely inactive in $\Delta mreC$ in contrast to the wild-type strain. However the promoter of *sopB* located in SPI-5 remained active but its activity was marginally lower than in the wild-type strain (Figure 3B). The regulation of many T3SS genes often require multiple signals for maximal expression and clearly other signals remain in the $\Delta mreC$ depletion mutant which drive expression of the SopB in SPI-5.

Expression of SPI-2 T3SS genes were monitored using a transcriptional reporter for the SPI-2 gene *ssaG*, whose promoter was cloned upstream of the *luxCDABE* luciferase operon in the plasmid pMK1-*lux* [52]. The construct was transformed into wild-type SL1344 and $\Delta mreC$, and the luminescence and OD600 measured during growth in SPI-2 inducing conditions (Figure 3B). The *ssaG* promoter remains active in the $\Delta mreC$ mutant although expression appears to be delayed, and is marginally less than in WT. This evidence supports the western blot data with α SseB and suggests that in contrast to the SPI-1 T3SS, the SPI-2 T3SS remains functional in the absence of the cytoskeleton.

Function of the RcsC Two-Component System in Regulation of SPI-1 T3S and Motility in $\Delta mreC$

Two-component regulatory systems are vital in sensing environmental and cell surface signals, enabling bacteria to rapidly adapt to ever changing conditions [53,54]. These signals are detected by histidine protein sensor kinases, which subsequently transfer phosphate groups to an aspartate residue in the response regulator proteins, thus modulating their regulatory activities. The environmental signals are thus transmitted by a phosphorelay system to regulate gene expression.

In order to identify putative regulators of the $\Delta mreC$ observed phenotypes, we have constructed knockout mutations in a range of two-component systems. As an initial screen, a panel of nine separate two-component system mutant strains were constructed as double mutants with $\Delta mreC$. One two-component system sensor kinase mutation $\Delta rcsC$ resulted in recovery of SPI-1 effector expression in the $\Delta mreC$ background as judged by western blotting using α SipC sera (Figure 5 panels A and B). Interestingly the amount of SipC protein expressed and secreted from the cell was less than the wild-type suggesting there are additional repressors continuing to operate (Figure 5 panels A and B and Figure S5). Furthermore, disruption of *rscC* also significantly de-repressed motility (Figure 6 and Figure S6) in a $\Delta mreC$ mutant similar to SPI-1 expression, again suggesting there are additional repressors involved. Expression of the RcsC protein *in trans* was able to restore the phenotype of $\Delta mreC \Delta rcsC$ back to the equivalent of a $\Delta mreC$

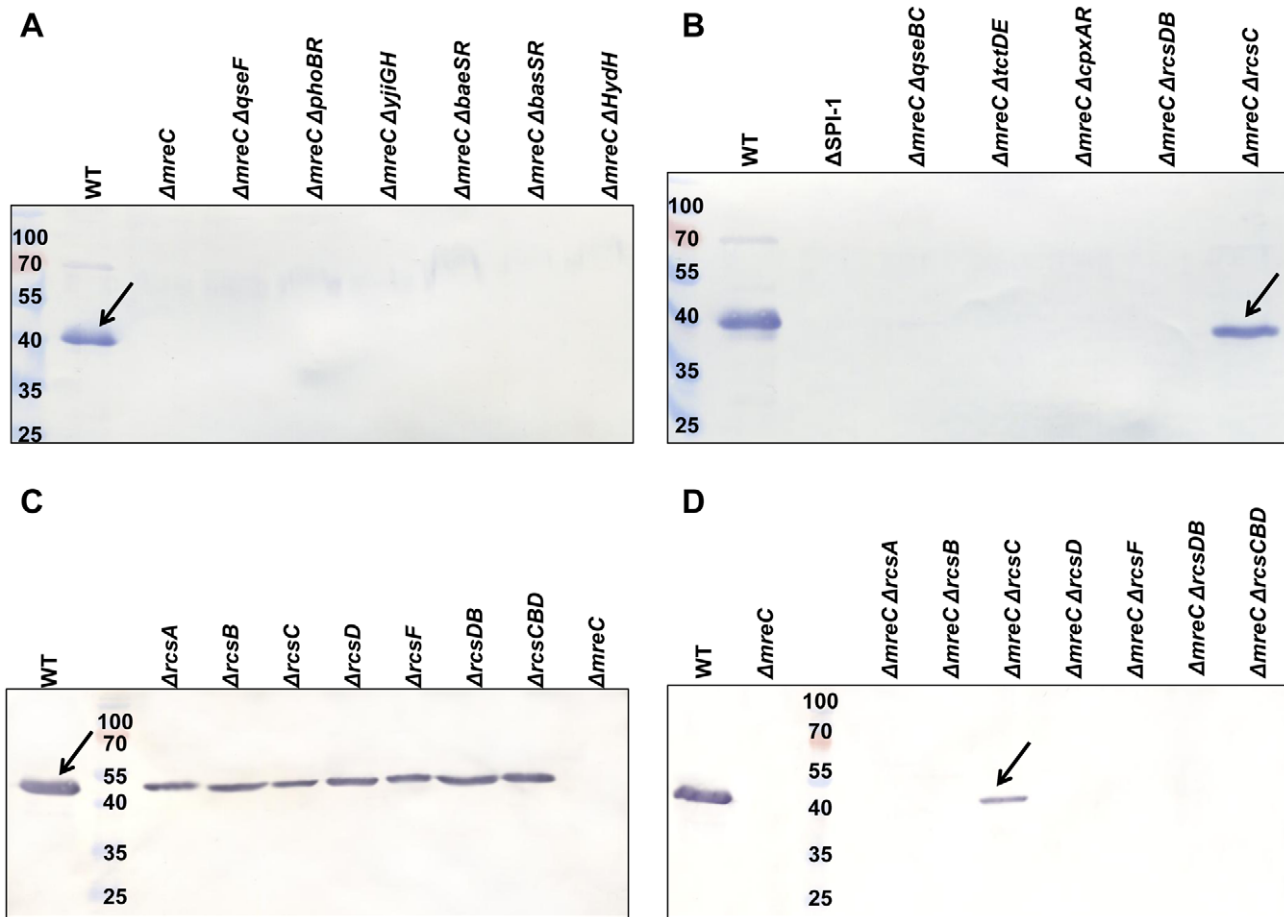


Figure 5. Western blotting screen of $\Delta mreC$ two-component system double mutants for recovery of SPI-1 T3S. Panels A and B show western blots of total protein samples obtained from SL1344 WT, $\Delta SPI-1$, $\Delta mreC$, $\Delta mreC \Delta qseF$, $\Delta mreC \Delta phoBR$, $\Delta mreC \Delta yjiGH$, $\Delta mreC \Delta baeSR$, $\Delta mreC \Delta basSR$, $\Delta mreC \Delta hydH$, $\Delta mreC \Delta qseBC$, $\Delta mreC \Delta tctDE$, $\Delta mreC \Delta cpxAR$, $\Delta mreC \Delta rcsDB$, and $\Delta mreC \Delta rcsC$ strains with $\alpha SipC$ antibody. Panels C and D show western blot of total protein samples obtained from SL1344 WT, $\Delta rcsA$, $\Delta rcsB$, $\Delta rcsC$, $\Delta rcsD$, $\Delta rcsF$, $\Delta rcsDB$, $\Delta rcsCBD$ and $\Delta mreC$ strains along with the $\Delta mreC \Delta rcsA$, $\Delta mreC \Delta rcsB$, $\Delta mreC \Delta rcsC$, $\Delta mreC \Delta rcsD$, $\Delta mreC \Delta rcsF$, $\Delta mreC \Delta rcsDB$, and $\Delta mreC \Delta rcsCBD$ double mutants with $\alpha SipC$ antibody. SipC is indicated at approximately 43kDa. doi:10.1371/journal.ppat.1002500.g005

strain, with respect to repressing SPI-1 type 3 secretion and motility. These complementation studies provide further evidence supporting the regulatory role of RcsC in the $\Delta mreC$ phenotypes (Figure S7).

Rcs is a highly complex multi-component phosphorelay system and was originally identified in regulating genes involved in capsule synthesis in *Escherichia coli* [55,56]. The RcsC sensor kinase phosphorylates RcsD, which subsequently phosphorylates the DNA binding response regulator RcsB. The unstable RcsA protein and additional auxillary proteins can also interact and regulate RcsB. The Rcs system is involved in down-regulating the expression of flagella, SPI-1 T3S and increasing biofilm formation [57].

We therefore also constructed $\Delta mreC \Delta rcsB$, $\Delta mreC \Delta rcsD$, $\Delta mreC \Delta rcsDB$ and $\Delta mreC \Delta rcsCBD$ mutants, which however did not restore either SPI-1 T3S or motility (Figures 5, 6, and S6). We propose that in the absence of RcsC signalling, phosphorylated levels of RcsB are depleted enabling de-repression of FlhDC and motility. The presence of RcsDB appears essential for restoring motility in the absence of RcsC [55]. The functionality of SPI-1 T3SS in the $\Delta mreC \Delta rcsC$ and $\Delta mreC \Delta rcsDB$ mutants were assessed in a TER assay, which revealed partial restoration of tight junction disruption in the $\Delta mreC \Delta rcsC$ mutant, but not in the $\Delta mreC \Delta rcsDB$ (Figure S8).

It has been suggested that the outer membrane protein RcsF may perceive some of the environmental signals necessary to

activate the Rcs phosphorelay system. To investigate this we constructed a $\Delta mreC \Delta rcsF$ mutant which failed to restore motility or SPI-1 T3S and appeared phenotypically identical to $\Delta mreC$ (Figure 5, S6). This would suggest that RcsF is not involved in the observed $\Delta mreC$ phenotypes. Furthermore as the auxillary protein RcsA can interact and regulate RcsB, we therefore disrupted the $rscA$ gene in $\Delta mreC$ and which also resulted in no impact on the observed phenotypes (Figure 5, S6).

In summary, we propose that RcsC is sensing cell surface perturbations [58] in $\Delta mreC$, resulting from a disrupted cytoskeleton, and subsequently down-regulating the expression of SPI-1 T3S and motility. This signalling appears to be independent of both RcsF and RcsA.

Chemical Genetic Inactivation of the Essential MreB Protein

A cell permeable compound named A22 [*S*-(3,4-Dichlorobenzyl) isothiourrea] has been demonstrated to perturb MreB function [59]. As an alternative approach to genetically disrupting the essential gene *mreB*, we exposed wild-type *Salmonella* cultures to A22 and observed a morphological change from rod to spherical-shaped cells. In addition we phenotypically screened and tested A22-treated cells for motility and T3S. The A22-treated cells were phenotyp-

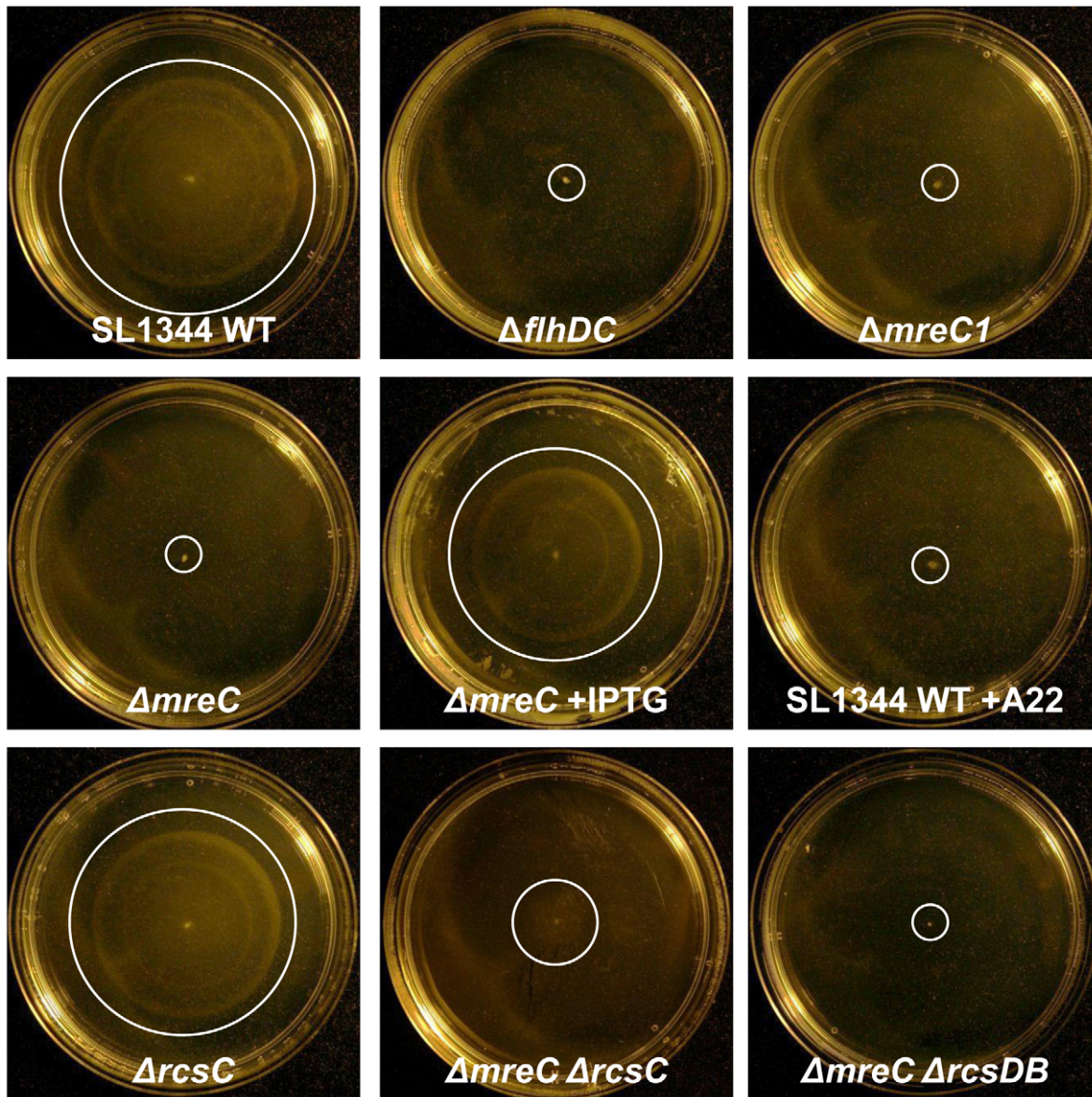


Figure 6. Motility of *Salmonella* mutant cells. Representative images showing the motility of SL1344 WT, $\Delta flhDC$ $\Delta mreC1$, $\Delta mreC$, $\Delta mreC$ plus IPTG, $\Delta rcsC$, $\Delta mreC \Delta rcsC$, $\Delta mreC \Delta rcsDB$, and SL1344 WT plus A22 cells grown on motility agar at 37°C. White circles highlight the limits of motility on the agar plates.

doi:10.1371/journal.ppat.1002500.g006

ically identical to $\Delta mreC$ with respect to cell shape, motility, SPI-1 T3S, and also SPI-2 T3S (data not shown). The effects of A22 were completely reversible following its removal (data not shown). Thus the chemical genetic inactivation of MreB, independently corroborates the phenotypic observations made with $\Delta mreC$.

The *Salmonella mre* Operon Plays an Important Role in Colonization during *in vivo* Infection

The $\Delta mreC$ defect clearly has an impact on the expression of important virulence determinants of *Salmonella in vitro*. We therefore wished to investigate the contribution of the bacterial cytoskeleton on the virulence of *Salmonella in vivo* using the mouse model. We observed that the SPI-1 T3SS in $\Delta mreC$ is completely down-regulated, and as this virulence system is important for infection through the oral route of inoculation the strain would be attenuated.

We therefore explored the colonization of $\Delta mreC$ using the intravenous route allowing us to examine the impact of the host on the further down-stream stages of infection. Groups of 5 female C57/BL6 mice were inoculated intravenously with *circa* 103 colony forming units of either control SL1344 or $\Delta mreC$. The times taken for clinical symptoms to appear were determined. Viable bacterial numbers in the spleen and liver for SL1344 were determined at days 1 and 4, and $\Delta mreC$ at days 1, 4, 7, and 10. The *in vivo* bacterial net growth curves vividly demonstrate two clear phenotypic effects upon the growth of $\Delta mreC$ compared to the wild-type. Firstly, there is a greater initial kill of $\Delta mreC$, and this is secondly followed by a slower net growth rate. However, in spite of the reduced growth rate of $\Delta mreC$, the bacterial numbers steadily increase over 6 days. This eventually causes the onset of clinical symptoms necessitating termination of the experiment at day 10 (Figure 7). During these stages *Salmonella* infect and multiply within macrophages and the

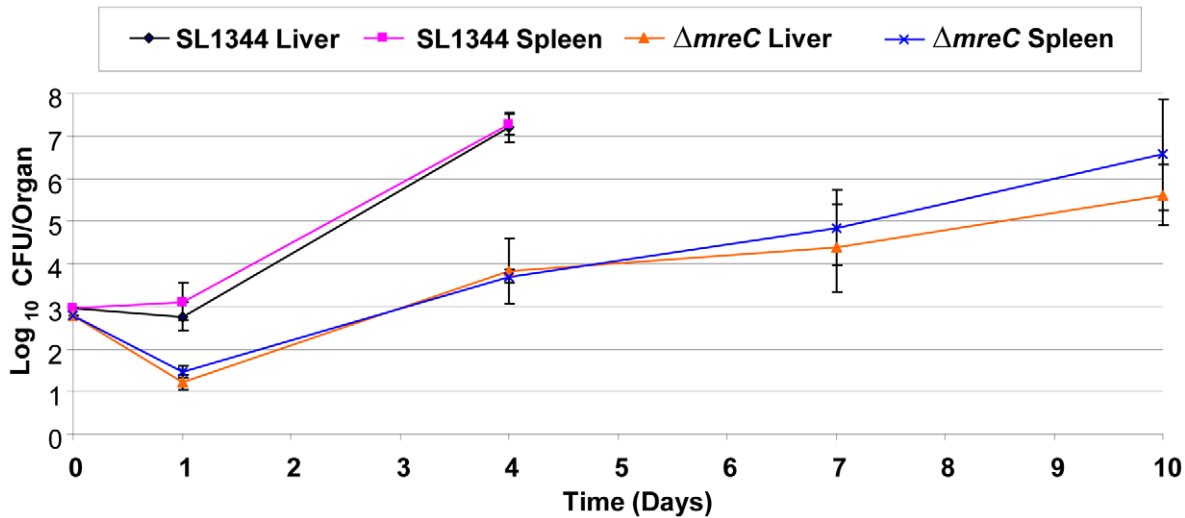


Figure 7. Contribution of $\Delta mreC$ to *in vivo* colonization. *In vivo* growth kinetics of WT SL1344 and $\Delta mreC$ in livers and spleens of C57BL/6 mice inoculated intravenously with 10^3 colony forming units. Viable bacterial counts in the spleen and liver were performed at days 1, 4, 7 and 10, and expressed as mean \log_{10} viable count \pm standard deviation. doi:10.1371/journal.ppat.1002500.g007

SPI-2 T3SS is essential for survival. Thus providing further evidence to support the presence of a functional SPI-2 T3SS in $\Delta mreC$. Collectively, these observations imply the *mreC* defect reduces the virulence of the strain, but does not completely abrogate its ability to multiply and cause disease systemically *in vivo*.

Morphology *in vivo*

Strains recovered from *in vivo* passage were tested for changes in morphology, motility and T3S, and were found to be identical to the input strain. Furthermore the *in vivo* morphology of the strain within livers and spleens was determined by immunofluorescence

microscopy. Sections of livers and spleens were taken and stained as described in the materials and methods. Figure 8 demonstrates the *Salmonella* $\Delta mreC$ mutant strain retains the round morphology *in vivo* compared to the rod shaped wild-type control. Collectively these data suggests that the mutation has remained stable during the *in vivo* passage for the virulence phenotypes tested.

Role of the Cytoskeleton in the Assembly, Regulation and Function of SPI-1 T3SS and Flagella

The regulation and assembly of SPI-1 T3SS and flagella are complex. When the bacterial cytoskeleton is disrupted both the

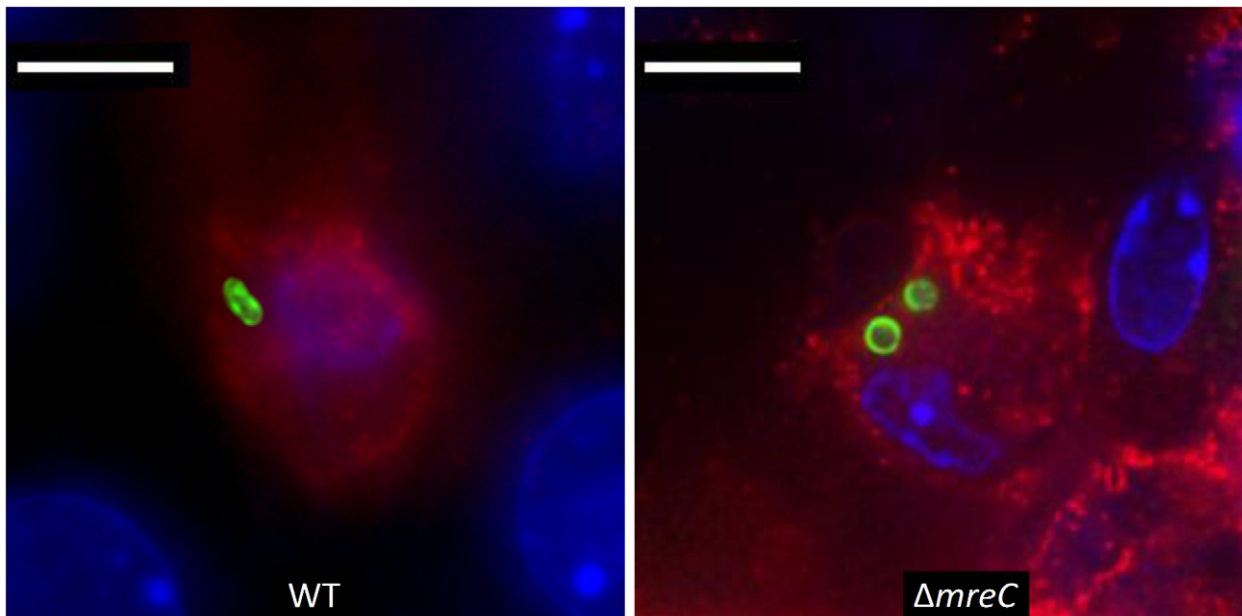


Figure 8. Morphology of $\Delta mreC$ in host tissues. Representative fluorescence micrograph of *Salmonella* SL1344 WT and $\Delta mreC$ within a phagocyte in infected livers of C57BL/6 mice at 72 h p.i. CD18+ expressing cells (red), *Salmonella* $\Delta mreC$ (green), nucleic acid is indicated by DAPI (blue). Scale bar, 5 μ m. doi:10.1371/journal.ppat.1002500.g008

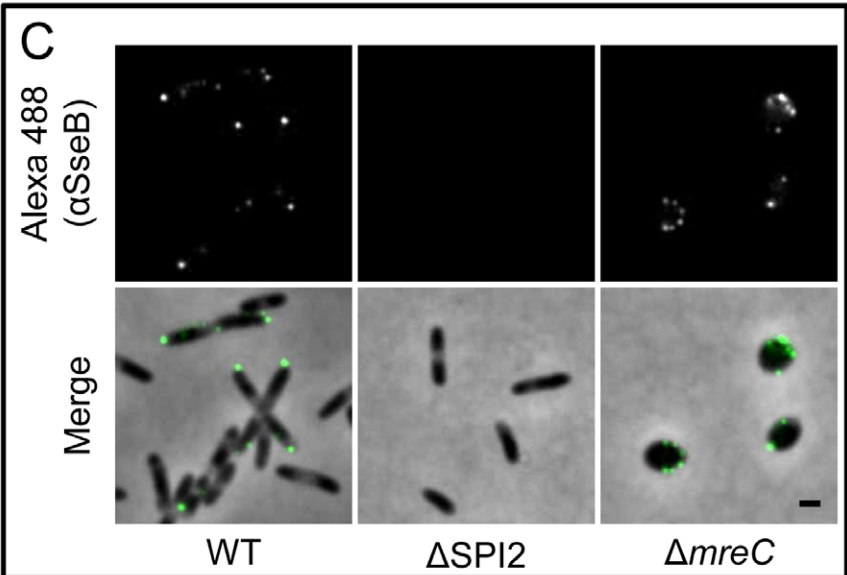
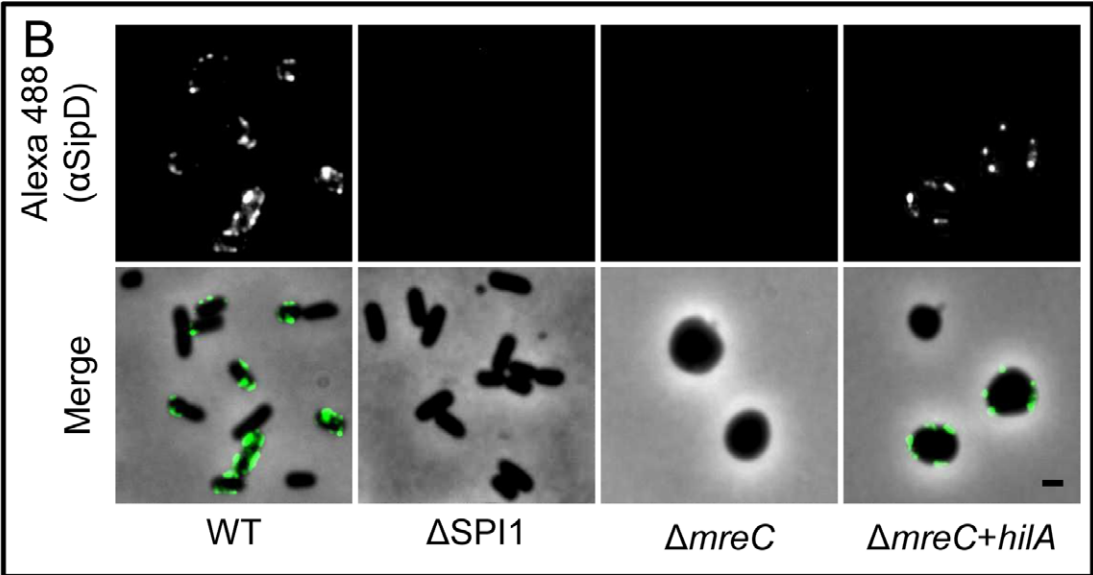
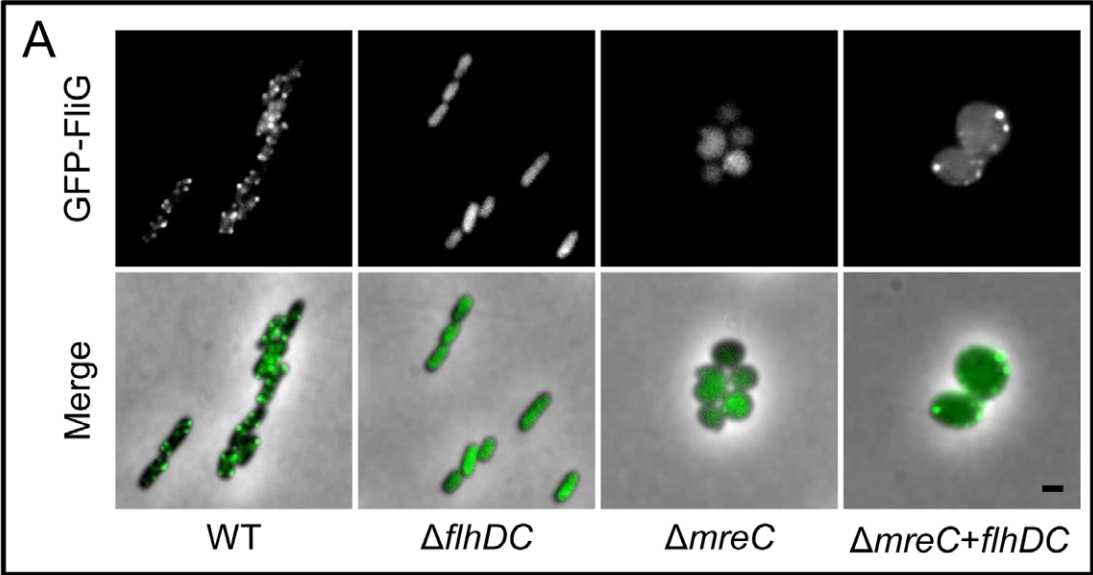


Figure 9. Localization of flagella and Type 3 secretion systems. Panel A shows representative images of *Salmonella* SL1344 WT, $\Delta flhDC$, $\Delta mreC$, and flagella-complemented $\Delta mreC$ pTET $flhDC$ cells. Panel B shows representative images of *Salmonella* SL1344 WT, $\Delta SPI1$, $\Delta mreC$, and SPI-1 complemented $\Delta mreC$ pBAD $hila$ cells. Panel C shows representative images of *Salmonella* SL1344 WT, $\Delta SPI2$, and $\Delta mreC$. Fluorescence images of (A) GFP-FliG, (B) Alexa488- α SipD or (C) Alexa488- α SseB (top panels) and phase merged images (bottom panels) are shown in each panel. Scale bar representing 1 μ m is indicated in the bottom right panel. doi:10.1371/journal.ppat.1002500.g009

SPI-1 T3SS and flagella expression are down-regulated. A hypothesis is that the integrity of the cytoskeleton is essential for the correct assembly of these complex macromolecular structures and in its absence the SPI-1 and flagella gene expression are down-regulated to conserve resources. Alternatively, in the absence of a functional cytoskeleton the bacterial cell is stressed and shuts down the expression of energetically expensive “non-essential” machinery. To test these ideas we wished to force on the expression of SPI-1 T3S and flagella genes, and examine whether these systems are correctly assembled and functional. We therefore expressed *in trans* from heterologous inducible promoters either the flagella master regulator FlhDC or the SPI-1 T3S regulator HilA in a panel of strains including $\Delta mreC$. Strikingly, expression of FlhDC restored both the expression and assembly of flagella on the cell surface as determined by fluorescence microscopy (Figure 9A) and motility assays (data not shown) in $\Delta mreC$. Furthermore, expression of HilA *in trans* up-regulated expression of the SPI-T3SS and its assembly on the cell surface as determined immunofluorescence microscopy (Figure 9B) western blotting with α SipB antibody (Figure S9) or functionally by TER measurements (Figure 4). In contrast to SPI-1 T3SS and flagella, the expression of the SPI-2 T3SS was not turned off in the $\Delta mreC$ mutant as shown in (Figure 9C). Interestingly, in WT cells the SPI-1 T3S apparatus and flagella appear to be present in around six to eight copies mainly along the long axis of the cell. In marked contrast the SPI-2 apparatus is typically present in one or two copies located at the poles of the bacterial cell [42], whereas their localisation appears less clear in the $\Delta mreC$ mutant, possibly due to perturbations in the cell envelope and the indistinct cell polarity in these cells caused by disruption of the cytoskeleton. The complementation of the functional assembly of SPI-1 T3SS was also confirmed using TER assays, where the levels of decrease in resistance after infection with $\Delta mreC$ strain reverted to that of the parent strain upon induction of the transcriptional regulator *hila* (Figure 9B and S9), or complementation of the $\Delta mreC$ mutation (Figure 4). Taken together the data support the notion that the cytoskeleton is not required for the correct assembly of these virulence factors but essential for their expression.

Discussion

Bacterial cells possess dynamic cytoskeletons composed of diverse classes of self-assembling polymeric proteins. Some of these proteins resemble eukaryotic actin, tubulin, and intermediate filaments both structurally and functionally [5,7,11,12]. The bacterial tubulin FtsZ plays a key role in cell division. Bacterial actins provide vital functions in maintaining cell morphology, segregating DNA, and positioning bacterial organelles. It has recently been demonstrated in *Helicobacter pylori*, that MreB is essential not for cell shape but for maintenance of the full enzymatic activity of urease, an essential virulence factor [60]. Furthermore the MreB cytoskeleton is also essential for the polar localisation of pili in *Pseudomonas aeruginosa* [61].

Using a variety of approaches we have demonstrated the importance of the bacterial cytoskeleton in the pathogenicity of *Salmonella*. MreC and MreD form a complex in the cytoplasmic membrane, which subsequently interacts with MreB. The *mreB*

gene appears to be essential in many organisms including as we discovered in *Salmonella*. Viable *mreB* mutants often contain compensatory changes in other genes e.g. *flsZ* which compensate for the lethality of the *mreB* lesion [37]. As an alternative strategy to investigate the function of the bacterial cytoskeleton and avoid these deleterious effects, we carefully constructed depletion mutants of *mreC* in strains harbouring a single-copy plasmid expressing the MreB operon from the *lac* promoter. In addition we confirmed the phenotypic effects of the *mreC* genetic lesion by disrupting the functions of MreB using a chemical genetics approach and inactivating MreB with A22.

Removal of the gratuitous inducer IPTG from the growth medium of the $\Delta mreC$ depletion mutant resulted in cells changing from rod to a spherical shaped morphology. Using fluorescence microscopy MreB was observed to be no longer distributed in a helical fashion throughout the cell but rather diffusely throughout the cytoplasm (data not shown). Presumably MreB polymers are no longer able to contact the cytoplasmic membrane via MreD attachment sites resulting in mis-assembly of the entire cytoskeleton. In growing cells, this disruption of the cytoskeleton leads to loss of the rod-shape.

We next examined the motility of $\Delta mreC$ depletion strain to assess the functionality of flagella. The strains were non-motile and western blotting revealed absence of the flagellin filament subunit proteins FliC and FliB in both secreted and also cytoplasmic protein fractions, suggesting expression of these alternative subunits had been switched off. Flagella gene expression is complex and involves a regulatory hierarchy of Class I, Class II, and Class III genes [38]. The class I *flhDC* operon is the master regulator, and FlhDC complex is required for transcriptional activation of the class II genes including the specialized flagellar sigma factor FliA. FliA alone or with FlhDC complex, activates expression of the class III operon genes encoding motor proteins, hook-associated proteins, the filament protein, and chemotaxis proteins [39,40]. Expression of the FlhDC complex was reduced but still appeared comparable between the wild-type and the $\Delta mreC$ suggesting changes in the promoter activity of *flhDC* alone are not responsible for the observed phenotype. Class II gene expression was significantly reduced. Expression of the Class III gene *fliC* was completely down-regulated confirming the western blot observations. Hence these independent observations are in accordance with the $\Delta mreC$ motility data. Thus in the absence of the cytoskeleton expression of class II and class III flagella genes appears to be down-regulated.

Expression of the SPI-1 T3S system is essential for invasion of intestinal epithelial cells and the SPI-2 T3SS plays a central role in survival within the hostile environment of a macrophage [43]. Western blotting revealed the SPI-1 T3S structural protein PrgH and the effectors SipA and SipC were no longer expressed or secreted in the $\Delta mreC$ depletion mutant. The phenotype was fully complementable by the addition of IPTG. Several environmental signals and transcriptional factors modulate expression of the SPI-1 and SPI-2 T3SS [43,45,62]. We wished to understand the mechanistic basis by which expression of the SPI-1-T3SS is down-regulated. Within SPI-1 there are key transcriptional activators which regulate expression of SPI-1 genes: HilC, HilD, HilA, and InvF. Using promoter-luciferase transcriptional reporter assays it

was revealed that the SPI-1 transcription factor gene promoters for *hilA*, *hilC*, *hilD*, and *invF* were completely inactive in $\Delta mrcC$, in marked contrast to the control wild-type strain. Surprisingly, the promoter of *sopB* located outside of SPI-1 in SPI-5 remained active but its activity was marginally lower than in the wild-type strain. The regulation of many T3SS genes often require the input of multiple signals for maximal expression and clearly other signals remain in the $\Delta mrcC$ depletion mutant which drive expression of the SopB in SPI-5. It therefore appears that the SPI-1 T3SS is completely down-regulated in the absence of a cytoskeleton by an unidentified regulatory factor. In contrast, the SPI-2 T3SS remains functional as evidenced by western blotting with SseB antibody and promoter-reporter assays. This is further corroborated with the *in vivo* evidence that following systemic inoculation, $\Delta mrcC$ is able to survive and multiply within the host. This takes place within the hostile environment of the macrophage where SPI-2 T3S is essential for biogenesis of the *Salmonella* containing vacuole and survival [43,63,64].

We wished to gain further insights into the mechanistic basis of the down-regulation of both SPI-1 T3SS and motility in $\Delta mrcC$. Two-component systems play an essential role in sensing and responding to environmental and cell surface signals [54]. To investigate if two-component systems contribute to the regulation of the $\Delta mrcC$ phenotypes, we constructed a panel of separate two-component system mutant strains in an $\Delta mrcC$ background. The double mutants were screened for recovery of motility and expression of the SPI-1 T3SS. A mutation in the *rscC* sensor kinase gene resulted in significant but not complete recovery of both motility and expression of the SPI-1 T3SS.

The Rcs phosphorelay system regulates a broad range of genes from capsule synthesis in *E. coli* to increasing biofilm formation [58]. RcsC also plays an important role in repressing expression of flagella and SPI-1 T3SS in *Salmonella* Typhi [57]. The RcsC sensor kinase normally phosphorylates RcsD, which subsequently phosphorylates the DNA binding response regulator RcsB. However, in $\Delta mrcC \Delta rcsDB$ and $\Delta mrcC \Delta rcsCBD$ there was no restoration of either motility or expression of the SPI-1 T3SS suggesting that RcsC signals repression and requires the presence of *rscDB* to mediate this effect. We propose that in $\Delta mrcC$, the sensor kinase RscC detects cell surface perturbations and down-regulates expression of flagella and the SPI-1 T3S apparatus [58]. This signalling is independent of both the outer membrane lipoprotein RcsF sensor and the auxiliary regulatory protein RcsA.

There are a number of explanations to provide a bacterial rationale for this shutdown in expression. In the absence of a functional cytoskeleton the flagella and SPI-1 T3SS are either not being correctly assembled, triggering a feedback loop to repress expression, or alternatively are down-regulated to prevent the cell from wasting valuable resources under these conditions. To test the assembly idea, we forced on the expression of flagella and SPI-1 T3SS genes by expressing the regulators *flhDC* or *hilA* *in trans* in $\Delta mrcC$. Using independent methods we observed the correct assembly and function of these macromolecular machines suggesting the cytoskeleton is not essential for functionality. The cytoskeleton could also have a role in sensing cellular stress, as has recently been suggested by Chiu and colleagues [65]. They propose that the integrity of the cytoskeleton may be exploited by the cell to monitor oxidative stress and physiological status. If the cytoskeleton disintegrates in the absence of MreC, this may be sensed by the cell leading to a shut-down of the SPI-1 T3S apparatus and down-regulation of flagella protein expression. We have provided mechanistic insights into the regulation of motility and SPI-1 T3S in $\Delta mrcC$. We have identified the two-component

system sensor RcsC as an important regulator controlling expression of these systems, presumably as a consequence of sensing membrane perturbations brought about by the disruption of the cytoskeleton [58].

With a non-functional SPI-1 T3SS, we would expect the $\Delta mrcC$ would be attenuated in mice when administered by the oral route as it is unable to invade intestinal epithelial cells by the SPI-1 T3SS. We therefore explored the colonization of $\Delta mrcC$ *in vivo* using the intravenous route of inoculation [66]. This provides an opportunity to examine the impact of $\Delta mrcC$ on the down-stream stages of infection. *Salmonella* infect and multiply within macrophages during the systemic stages of infection. Survival within the hostile environment of the macrophage would require a functional SPI-2 T3SS in the *Salmonella*-containing vacuole to remodel the host cell environment and survive attack from reactive oxygen free radicals [64,67,68]. By examining the *in vivo* net bacterial growth curves within livers and spleens two clear phenotypic effects were revealed with $\Delta mrcC$ compared to the wild-type. Greater initial killing of $\Delta mrcC$ is followed by a slower net growth rate with the bacterial numbers steadily increasing over six days. Clinical symptoms begin to appear and by day ten these symptoms necessitate termination of the experiment. The phenotypic data clearly imply the $\Delta mrcC$ defect reduces the colonization of *Salmonella*, but does not completely abrogate its ability to multiply and cause disease systemically *in vivo*. This would suggest that the second T3S in *Salmonella* encoded on SPI-2 remains sufficiently functional to permit growth in the absence of the cytoskeleton.

In the absence of an intact cytoskeleton in $\Delta mrcC$ the expression of the SPI-1 T3SS and flagella are clearly down-regulated. Strikingly however, the SPI-2 T3SS appears to remain functional contributing to the virulence of the $\Delta mrcC$ strain observed *in vivo*. A possible explanation could be that the regulation of the SPI-2 T3SS is co-ordinated independently of the integrity of the cytoskeleton in contrast to flagella and SPI-1 T3SS. Collectively these data highlight the importance of the bacterial cytoskeleton in the ability of *Salmonella* to cause disease, and may provide opportunities for the development of new antimicrobials to target the cytoskeleton.

Supporting Information

Figure S1 Expression of MreC in complemented $\Delta mrcC$ cells. Western blot of total protein samples from SL1344 WT, $\Delta mrcC1$, $\Delta mrcC$, and $\Delta mrcC$ plus 100 μ M IPTG cells using α MreC antibody. MreC is indicated at approximately 38kDa and is distinguishable from background bands.

(TIF)

Figure S2 Growth curve of *Salmonella* mutant cells. Log phase growth of SL1344 WT, $\Delta mrcC1$, $\Delta mrcC$, $\Delta mrcC$ plus 100 μ M IPTG, and A22 treated SL1344 WT cells. Strains were grown in LB media at 37°C.

(TIF)

Figure S3 Motility of *Salmonella* Δmrc mutant cells. Motility of SL1344 WT, $\Delta flhDC$, $\Delta mrcC1$, $\Delta mrcC$, $\Delta mrcC$ plus 100 μ M IPTG, and A22 treated SL1344 WT shown as a percentage of the wild type. Strains were grown on motility agar at 37°C. Experiments were repeated at least three times and error bars indicate SD. * Indicates statistical difference from WT ($p < 0.05$).

(TIF)

Figure S4 Translocation of SipB SPI-1 effector protein into Caco-2 cells. Western blot of host cytosol fractions with α SipB antibody following infection of cells with *Salmonella*

SL1344 WT, Δ SPI-1, Δ mreC1, Δ mreC (+/- IPTG) mutants. SipB is indicated at approximately 65kDa. (TIF)

Figure S5 Secretion of SPI-1 effector protein SipC in Δ rcsC mutant cells. Western blot of secreted protein samples from SL1344 WT, Δ mreC, Δ SPI-1, Δ SPI-2, Δ rcsC, and Δ mreC Δ rcsC cells using α SipC antibody. SipC is indicated at approximately 43kDa. (TIF)

Figure S6 Motility of Salmonella Δ rcs mutant cells. Motility of SL1344 WT, Δ mreC, Δ flhDC, Δ rcsA, Δ rcsB, Δ rcsC, Δ rcsD, Δ rcsF, Δ rcsDB, Δ rcsCBD, Δ mreC Δ rcsA, Δ mreC Δ rcsB, Δ mreC Δ rcsC, Δ mreC Δ rcsD, Δ mreC Δ rcsF, Δ mreC Δ rcsDB, and Δ mreC Δ rcsCBD cells shown as a percentage of the wild type. Experiments were repeated at least three times and error bars indicate SD. Strains were grown on motility agar at 37°C. (TIF)

Figure S7 Effect of rcsC expression on SipC production and motility. Panels A and B show western blots from SL1344 WT, mreC, and SPI-1 control strains, and SL1344 WT pBADrcsC, mreC pBADrcsC, rcsC pBADrcsC, and mreC rcsC pBADrcsC strains (+/- arabinose) with α SipC antibody. SipC is indicated at approximately 43kDa. Panel C shows motility of SL1344 WT, mreC, SL1344 WT pBADrcsC, mreC pBADrcsC, rcsC pBADrcsC, and mreC rcsC pBADrcsC strains (+/- arabinose) shown as a percentage of the wild type. Experiments were repeated at least three times and error bars indicate standard deviation. (TIF)

Figure S8 Percentage change in transepithelial resistance of differentiated Caco-2 cells after 4hr infection with Δ rcs mutant strains. TER of polarised Caco-2

monolayers exposed to *Salmonella* strains at an MOI of 20. TER change is expressed as a percentage alteration at 4hr compared to the initial value at time zero. Error bars indicate the standard deviations derived from at least three independent experiments. * Indicates statistical difference from WT ($p < 0.05$). (TIF)

Figure S9 Complementation of Salmonella Pathogenicity Island SPI-1 in Δ mreC mutant. Expression of SPI-1 proteins in WT SL1344, Δ SPI-1, and Δ mreC mutants, and complemented Δ mreC pBADhila strain during SPI-1 inducing conditions as revealed by western blotting with polyclonal α SipB antibody. SipB is indicated at approximately 63kDa, and a breakdown product is evident. (TIF)

Acknowledgments

We are grateful to the anonymous reviewers of the manuscript for their comments and suggestions. We would like to thank Brian Ahmer and Ivan Rychlik for their generous gifts of the flagella and SPI-1 T3SS promoter-reporter plasmid sets. In addition we would like to thank Roberto La Ragona for the flagella antibodies; Purva Vats and Lawrence Rothfield for the pLE7 plasmid; Keiichi Namba and Tooru Minamino for the *fliG-gfp* strain, Alex Faulds-Pain and Phil Aldridge for the Δ flhDC strain, Waldemar Vollmer for the MreC antibodies, and also Xiu-Jun Yu and David Holden for the SseB antibodies and the *DssaV* strain. We also wish to thank Jeff Errington, Kenn Gerdes, David Holden, David Clarke, and Simon Andrews for valuable discussions.

Author Contributions

Conceived and designed the experiments: DMB AJG PD PM CMAK. Performed the experiments: DMB LK AJG PD FJEM. Analyzed the data: DMB MHK ACD AJG PD PM CMAK. Contributed reagents/materials/analysis tools: EJM VK RAD. Wrote the paper: DMB CMAK.

References

- Pang T, Levine MM, Ivanoff B, Wain J, Finlay BB (1998) Typhoid fever—important issues still remain. *Trends Microbiol* 6: 131–133.
- Lilic M, Galkin VE, Orlova A, VanLoock MS, Egelman EH, et al. (2003) Salmonella SipA polymerizes actin by stapling filaments with nonglobular protein arms. *Science* 301: 1918–1921.
- Piddock LJ (2006) Multidrug-resistance efflux pumps - not just for resistance. *Nat Rev Microbiol* 4: 629–636.
- Mirza SH, Beeching NJ, Hart CA (1996) Multi-drug resistant typhoid: a global problem. *J Med Microbiol* 44: 317–319.
- Jones LJ, Carballido-Lopez R, Errington J (2001) Control of cell shape in bacteria: helical, actin-like filaments in *Bacillus subtilis*. *Cell* 104: 913–922.
- Bi E, Lutkenhaus J (1991) FtsZ ring structure associated with division in *Escherichia coli*. *Nature* 354: 161–164.
- Lowe J, Amos LA (1998) Crystal structure of the bacterial cell-division protein FtsZ. *Nature* 391: 203–206.
- Lutkenhaus J, Addinall SG (1997) Bacterial cell division and the Z ring. *Annu Rev Biochem* 66: 93–116.
- Ausmees N, Kuhn JR, Jacobs-Wagner C (2003) The bacterial cytoskeleton: An intermediate filament-like function. *Cell* 115: 705–713.
- Carballido-Lopez R, Errington J (2003) A dynamic bacterial cytoskeleton. *Trends Cell Biol* 13: 577–583.
- van den Ent F, Amos L, Löwe J (2001) Bacterial ancestry of actin and tubulin. *Curr Opin Microbiol* 4: 634–638.
- van den Ent F, Amos LA, Löwe J (2001) Prokaryotic origin of the actin cytoskeleton. *Nature* 413: 39–44.
- Kruse T, Bork-Jensen J, Gerdes K (2005) The morphogenetic MreBCD proteins of *Escherichia coli* form an essential membrane-bound complex. *Mol Microbiol* 55: 78–89.
- Kruse T, Moller-Jensen J, Lobner-Olesen A, Gerdes K (2003) Dysfunctional MreB inhibits chromosome segregation in *Escherichia coli*. *EMBO J* 22: 5283–5292.
- Formstone A, Errington J (2005) A magnesium-dependent mreB null mutant: implications for the role of mreB in *Bacillus subtilis*. *Mol Microbiol* 55: 1646–1657.
- Gitai Z, Dye N, Shapiro L (2004) An actin-like gene can determine cell polarity in bacteria. *Proc Natl Acad Sci U S A* 101: 8643–8648.
- Figge RM, Divakaruni AV, Gober JW (2004) MreB, the cell shape-determining bacterial actin homologue, co-ordinates cell wall morphogenesis in *Caulobacter crescentus*. *Mol Microbiol* 51: 1321–1332.
- Wachi M, Doi M, Okada Y, Matsushashi M (1989) New Mre Genes Mrec and Mred, Responsible for Formation of the Rod Shape of *Escherichia-Coli*-Cells. *J Bacteriol* 171: 6511–6516.
- Divakaruni AV, Loo RRO, Xie Y, Loo JA, Gober JW (2005) The cell-shape protein MreC interacts with extracytoplasmic proteins including cell wall assembly complexes in *Caulobacter crescentus*. *Proc Natl Acad Sci U S A* 102: 18602–18607.
- Vats P, Shih YL, Rothfield L (2009) Assembly of the MreB-associated cytoskeletal ring of *Escherichia coli*. *Mol Microbiol* 72: 170–82.
- Slovak PM, Porter SL, Armitage JP (2006) Differential localization of Mre proteins with BBP2 in *Rhodobacter sphaeroides*. *J Bacteriol* 188: 1691–1700.
- Gitai Z, Dye NA, Reisenauer A, Wachi M, Shapiro L (2005) MreB actin-mediated segregation of a specific region of a bacterial chromosome. *Cell* 120: 328–341.
- Madabhushi R, Mariani KJ (2009) Actin homolog MreB affects chromosome segregation by regulating topoisomerase IV in *Escherichia coli*. *Mol Cell* 33: 171–180.
- Kruse T, Blagoev B, Lobner-Olesen A, Wachi M, Sasaki K, et al. (2006) Actin homolog MreB and RNA polymerase interact and are both required for chromosome segregation in *Escherichia coli*. *Genes Dev* 20: 113–124.
- Shiomi D, Sakai M, Niki H (2008) Determination of bacterial rod shape by a novel cytoskeletal membrane protein. *EMBO J* 27: 3081–3091.
- Bendezu FO, Hale CA, Bernhardt TG, de Boer PA (2009) RodZ (YfgA) is required for proper assembly of the MreB actin cytoskeleton and cell shape in *E. coli*. *EMBO J* 28: 193–204.
- Alyahya SA, Alexander R, Costa T, Henriques AO, Emonet T, et al. (2009) RodZ, a component of the bacterial core morphogenic apparatus. *Proc Natl Acad Sci U S A* 106: 1239–1244.
- Ghosh AS, Young KD (2005) Helical Disposition of Proteins and Lipopolysaccharide in the Outer Membrane of *Escherichia coli*. *J Bacteriol* 187: 1913–1922.
- Taghbalout A, Rothfield L (2008) RNaseE and RNA helicase B play central roles in the cytoskeletal organization of the RNA degradosome. *J Biol Chem* 283: 13850–13855. M709118200 [pii];10.1074/jbc.M709118200 [doi].

30. Ehrbar K, Mirol S, Friebe A, Stender S, Hardt WD (2002) Characterization of effector proteins translocated via the SPI1 type III secretion system of *Salmonella typhimurium*. *Int J Med Microbiol* 291: 479–485.
31. Datsenko KA, Wanner BL (2000) One-step inactivation of chromosomal genes in *Escherichia coli* K-12 using PCR products. *Proc Natl Acad Sci U S A* 97: 6640–6645. 10.1073/pnas.120163297 [doi];120163297 [pii].
32. Morimoto YV, Nakamura S, Kami-ike N, Namba K, Minamino T (2010) Charged residues in the cytoplasmic loop of MotA are required for stator assembly into the bacterial flagellar motor. *Mol Microbiol* 78: 1117–1129.
33. Karlinsky JE, Tanaka S, Bettenworth V, Yamaguchi S, Boos W, et al. (2000) Completion of the hook-basal body complex of the *Salmonella typhimurium* flagellum is coupled to FlgM secretion and flhC transcription. *Mol Microbiol* 37: 1220–1231.
34. Dean P, Kenny B (2004) Intestinal barrier dysfunction by enteropathogenic *Escherichia coli* is mediated by two effector molecules and a bacterial surface protein. *Mol Microbiol* 54: 665–675.
35. McClelland M, Sanderson KE, Spieth J, Clifton SW, Latreille P, et al. (2001) Complete genome sequence of *Salmonella enterica* serovar Typhimurium LT2. *Nature* 413: 852–856.
36. Shih YL, Le T, Rothfield L (2003) Division site selection in *Escherichia coli* involves dynamic redistribution of Min proteins within coiled structures that extend between the two cell poles. *Proc Natl Acad Sci USA* 100: 7865–7870. 10.1073/pnas.1232225100 [doi];1232225100 [pii].
37. Bendezu FO, de Boer PAJ (2008) Conditional Lethality, Division Defects, Membrane Involution, and Endocytosis in mre and mrd Shape Mutants of *Escherichia coli*. *J Bacteriol* 190: 1792–1811.
38. Macnab RM (2003) How bacteria assemble flagella. *Ann Rev Microbiol* 57: 77–100. DOI 10.1146/annurev.micro.57.030502.090832.
39. Kameda Y (1982) Fusions of flagellar operons to lactose genes on a mu lac bacteriophage. *J Bacteriol* 150: 16–26.
40. Kutsukake K, Ohya Y, Iino T (1990) Transcriptional analysis of the flagellar regulon of *Salmonella typhimurium*. *J Bacteriol* 172: 741–747.
41. Goodier RI, Ahmer BM (2001) SirA orthologs affect both motility and virulence. *J Bacteriol* 183: 2249–2258.
42. Chakravorty D, Rohde M, Jager L, Deiwick J, Hensel M (2005) Formation of a novel surface structure encoded by *Salmonella* Pathogenicity Island 2. *EMBO J* 24: 2043–2052.
43. Waterman SR, Holden DW (2003) Functions and effectors of the *Salmonella* pathogenicity island 2 type III secretion system. *Cell Microbiol* 5: 501–511.
44. Espina M, Olive AJ, Kenjale R, Moore DS, Ausar SF, et al. (2006) IpaD Localizes to the Tip of the Type III Secretion System Needle of *Shigella flexneri*. *Infect Immun* 74: 4391–4400.
45. Galan JE, Wolf-Watz H (2006) Protein delivery into eukaryotic cells by type III secretion machines. *Nature* 444: 567–573.
46. Karavolos MH, Roe AJ, Wilson M, Henderson J, Lee JJ, et al. (2005) Type III secretion of the *Salmonella* effector protein SopE is mediated via an N-terminal amino acid signal and not an mRNA sequence. *J Bacteriol* 187: 1559–1567.
47. Lucas RL, Lee CA (2001) Roles of hilC and hilD in regulation of hilA expression in *Salmonella enterica* serovar Typhimurium. *J Bacteriol* 183: 2733–2745.
48. Ellermeier CD, Ellermeier JR, Schlauch JM (2005) HilD, HilC and RtsA constitute a feed forward loop that controls expression of the SPI1 type three secretion system regulator hilA in *Salmonella enterica* serovar Typhimurium. *Mol Microbiol* 57: 691–705.
49. Papezova K, Gregorova D, Jonuschies J, Rychlik I (2007) Ordered expression of virulence genes in *Salmonella enterica* serovar typhimurium. *Folia Microbiol* 52: 107–114.
50. Winson MK, Swift S, Fish L, Throup JP, Jorgensen F, et al. (1998) Construction and analysis of luxCDABE-based plasmid sensors for investigating N-acyl homoserine lactone-mediated quorum sensing. *FEMS Microbiol Lett* 163: 185–192.
51. Winson MK, Swift S, Hill PJ, Sims CM, Griesmayr G, et al. (1998) Engineering the luxCDABE genes from *Photobacterium luminescens* to provide a bioluminescent reporter for constitutive and promoter probe plasmids and mini-Tn5 constructs. *FEMS Microbiol Lett* 163: 193–202.
52. Karavolos MH, Spencer H, Bulmer DM, Thompson A, Winzer K, et al. (2008) Adrenaline modulates the global transcriptional profile of *Salmonella* revealing a role in the antimicrobial peptide and oxidative stress resistance responses. *BMC Genomics* 9: 458. 1471-2164-9-458 [pii];10.1186/1471-2164-9-458 [doi].
53. Krell T, Lacal J, Busch A, Silva-Jimenez H, Guazzaroni ME, et al. (2010) Bacterial sensor kinases: diversity in the recognition of environmental signals. *Annu Rev Microbiol* 64: 539–559.
54. Stock AM, Robinson VL, Goudreau PN (2000) Two-component signal transduction. *Annu Rev Biochem* 69: 183–215.
55. Clarke DJ (2010) The Rcs phosphorelay: more than just a two-component pathway. *Future Microbiol* 5: 1173–1184.
56. Pescaretti ML, Lopez FE, Morero RD, Delgado MA (2010) Transcriptional autoregulation of the RcsCDB phosphorelay system in *Salmonella enterica* serovar Typhimurium. *Microbiology* 156: 3513–3521.
57. Arricau N, Hermant D, Waxin H, Ecobichon C, Duffey PS, et al. (1998) The RcsB-RcsC regulatory system of *Salmonella typhi* differentially modulates the expression of invasion proteins, flagellin and Vi antigen in response to osmolarity. *Mol Microbiol* 29: 835–850.
58. Majdalani N, Gottesman S (2005) The Rcs phosphorelay: a complex signal transduction system. *Annu Rev Microbiol* 59: 379–405.
59. Iwai N, Nagai K, Wachi M (2002) Novel S-benzylisothiourea compound that induces spherical cells in *Escherichia coli* probably by acting on a rod-shape-determining protein(s) other than penicillin-binding protein 2. *Biosci Biotechnol Biochem* 66: 2658–2662.
60. Waidner B, Specht M, Dempwolff F, Haeblerer K, Schaetzle S, et al. (2009) A novel system of cytoskeletal elements in the human pathogen *Helicobacter pylori*. *PLoS Pathog* 5: e1000669.
61. Cowles KN, Gitai Z (2010) Surface association and the MreB cytoskeleton regulate pilus production, localization and function in *Pseudomonas aeruginosa*. *Mol Microbiol* 76: 1411–1426.
62. Lober S, Jackel D, Kaiser N, Hensel M (2006) Regulation of *Salmonella* pathogenicity island 2 genes by independent environmental signals. *Int J Med Microbiol* 296: 435–447.
63. Hensel M (2000) *Salmonella* pathogenicity island 2. *Mol Microbiol* 36: 1015–1023.
64. Hensel M, Shea JE, Waterman SR, Mundy R, Nikolaus T, et al. (1998) Genes encoding putative effector proteins of the type III secretion system of *Salmonella* pathogenicity island 2 are required for bacterial virulence and proliferation in macrophages. *Mol Microbiol* 30: 163–174.
65. Chiu S-W, Chen S-Y, Wong H (2008) Localization and Expression of MreB in *Vibrio parahaemolyticus* under Different Stresses. *Appl Environ Microbiol* 74: 7016–7022.
66. Hormaeche CE (1979) Genetics of Natural-Resistance to *Salmonellae* in Mice. *Immunology* 37: 319–327.
67. Shea JE, Beuzon CR, Gleeson C, Mundy R, Holden DW (1999) Influence of the *Salmonella typhimurium* pathogenicity island 2 type III secretion system on bacterial growth in the mouse. *Infect Immun* 67: 213–219.
68. Vazquez-Torres A, Xu Y, Jones-Carson J, Holden DW, Lucia SM, et al. (2000) *Salmonella* pathogenicity island 2-dependent evasion of the phagocyte NADPH oxidase. *Science* 287: 1655–8.
69. Hoiseth SK, Stocker BA (1981) Aromatic-dependent *Salmonella typhimurium* are non-virulent and effective as live vaccines. *Nature* 291: 238–239.
70. Murray RA, Lee CA (2000) Invasion genes are not required for *Salmonella enterica* serovar typhimurium to breach the intestinal epithelium: evidence that salmonella pathogenicity island 1 has alternative functions during infection. *Infect Immun* 68: 5050–5055.
71. Beuzon CR, Salcedo SP, Holden DW (2002) Growth and killing of a *Salmonella enterica* serovar Typhimurium sifA mutant strain in the cytosol of different host cell lines. *Microbiology* 148: 2705–2715.
72. Faulds-Pain, AK (2008) The Regulation of Flagellar Filament Assembly in *Caulobacter Crescentus* [dissertation]. Newcastle University.
73. Bolivar F (1978) Construction and characterization of new cloning vehicles. III. Derivatives of plasmid pBR322 carrying unique Eco RI sites for selection of Eco RI generated recombinant DNA molecules. *Gene* 4: 121–136. 0378-1119(78)90025-2 [pii].
74. Sutcliffe JG (1979) Complete nucleotide sequence of the *Escherichia coli* plasmid pBR322. *Cold Spring Harbor Symp Quant Biol* 43 Pt 1: 77–90.
75. Guzman LM, Belin D, Carson MJ, Beckwith J (1995) Tight regulation, modulation, and high-level expression by vectors containing the arabinose PBAD promoter. *J Bacteriol* 177: 4121–4130.
76. Hautefort I, Proenca MJ, Hinton JC (2003) Single-copy green fluorescent protein gene fusions allow accurate measurement of *Salmonella* gene expression in vitro and during infection of mammalian cells. *Appl Environ Microbiol* 69: 7480–7491.
77. Gottfredsen M, Gerdes K (1998) The *Escherichia coli* relBE genes belong to a new toxin antitoxin gene family. *Mol Microbiol* 29: 1065–1076.